EMPLOYMENT OF DUAL FREQUENCY EXCITATION METHOD TO IMPROVE THE ACCURACY OF AN OPTICAL CURRENT SENSOR, BY MEASURING BOTH CURRENT AND TEMPERATURE

Avinash Karri

Thesis Prepared for the Degree of

MASTER OF SCIENCE

UNIVERSITY OF NORTH TEXAS

December 2008

APPROVED:

Shuping Wang, Major Professor
Parthasarathy Guturu, Minor Professor
Hai Deng, Committee Member
Murali Varanasi, Chair of the Department of Electrical Engineering
Costas Tsatsoulis, Dean of the College of Engineering
Sandra L. Terrell, Dean of the Robert B. Toulouse School of Graduate Studies

Karri, Avinash. Employment of dual frequency excitation method to improve the accuracy of an optical current sensor, by measuring both current and temperature. Master of Science (Electrical Engineering), December 2008, 94 pp., 6 tables, 25 illustrations, references, 35 titles.

Optical current sensors (OCSs) are initially developed to measure relatively large current over a wide range of frequency band. They are also used as protective devices in the event a fault occurs due to a short circuit, in the power generation and distribution industries. The basic principal used in OCS is the Faraday effect. When a light guiding faraday medium is placed in a magnetic field which is produced by the current flowing in the conductor around the magnetic core, the plane of polarization of the linearly polarized light is rotated. The angle of rotation is proportional to the magnetic field strength, proportionality constant and the interaction length. The proportionality constant is the Verdet constant V (λ, T), which is dependent on both temperature and wavelength of the light. Opto electrical methods are used to measure the angle of rotation of the polarization plane. By measuring the angle the current flowing in the current carrying conductor can be calculated. But the accuracy of the OCS is lost of the angle of rotation of the polarization plane is dependent on the Verdet constant, apart from the magnetic field strength. As temperature increases the Verdet constant decreases, so the angle of rotation decreases. To compensate the effect of temperature on the OCS, a new method has been proposed.

The current and temperature are measured with the help of a duel frequency method. To detect the line current in the conductor or coil, a small signal from the line current is fed to the reference of the lock in. To detect the temperature, the coil is excited with an electrical signal of a frequency different from the line frequency, and a small sample of this frequency signal is

applied to the reference of the lock in. The temperature and current readings obtained are look up at the database value to give the actual output. Controlled environment is maintained to record the values in the database that maps the current and temperature magnitude values at the DSP lock in amplifier, to the actual temperature and current. By this method we can achieve better compensation to the temperature changes, with a large dynamic range and better sensitivity and accuracy.

ACKNOWLEDGEMENTS

First, I am very thankful to Shuping Wang, under whose able direction the thesis work has been conducted. Without her suggestions and guidance this project would not have taken this form. I would also like to thank Yossi Harlev, Len Jhonson and Optisense Network Inc, for their guidance and funding the project partly. I would also like to thank my committee members Parthasarathy Guturu and Hai Deng for reviewing my thesis.

TABLE OF CONTENTS

Page

LIST OF TABLES

Page

LIST OF FIGURES

Page

CHAPTER 1

INTRODUCTION

1.1 Introduction

Since few decades, optical current sensors (OCS) are gaining popularity to the conventional current transformers (CT) in the power industry for measuring high order currents. OCSs offer advantages in cost, safety and performance.

Conventionally, wire wound current CTs were used to measure the current in a conductor. The secondary current of the CT is used for either metering or protective devices. Normally the secondary current is in the order of 5A, which is converted into voltage for the digital signal processing. But during a short circuits fault on the power system the current magnitude in the secondary will be increased by as much as 10 times. This large current may cause noise in the digital electronic devices. At higher currents the magnetic flux density of the CT core may become saturated, and so it affects the linearity.

The OCS was initially developed to measure relatively large current over a wide range of frequency band. They are also used as protective devices in the event a fault occurs due to a short circuit, in the power generation and distribution industries. The OCS has several advantages when compared to the conventional iron core wire wound CTs. The OCSs offer electrical isolation, as there is no direct contact with the electrical conductor. The OCSs possess higher dynamic range over large frequencies, exhibit more linear response with zero hysteresis when compared to the conventional iron core CTs.

The OCSs are light and compact, and consumes very less power for their operation. So there is no chance of explosion and are hence safe.

The basic principal used in OCS is the Faraday effect. When a light guiding Faraday medium is placed in a magnetic field which is produced by the current flowing in the conductor around the magnetic core, the plane of polarization of the linearly polarized light is rotated. The angle of rotation is proportional to the magnetic field strength, proportionality constant and the interaction length. The proportionality constant is the Verdet constant V (λ, T), which is dependent on both temperature [1, 4] and wavelength of the light [2]. Opto electrical methods are used to measure the angle of rotation of the polarization plane. By measuring the angle the current flowing in the current carrying conductor can be calculated.

1.2 Purpose, Motivation and Objective of Study

Considerable research has been conducted on OCSs, and some have been implemented. A few major classes of OCSs [3] are conventional CT with optical readout, magnetic concentrator with optical measurement, optical path surrounding conductor using bulk glass, and optical path surrounding conductor using an optical fiber cable and using a witness sensor. Of the above methods the magnetic concentrator with optical measurement has advantages that it is immune to electromagnetic interference from nearby current carriers and only a small amount of optical material is needed [5]. To improve the sensitivity of the sensor further various techniques are used. The path length of the light is increased by multiple reflections inside the Faraday crystal [6] and by

reducing the gap length which in turn will yield in more magnetic fields across the air gap and so more Faraday rotation [7].

But the desired accuracy cannot be still attained as the current measurement is dependent on Verdet constant and a change in the temperature will alter the current measurements, so it affects the sensitivity of the OCS. As mentions above the angle of rotation of the linearly polarized light depends on the magnetic field strength, interaction length and Verdet constant that is dependent on both temperate and wavelength. To make a highly sensitive and accurate current device, we have to design the OCS, such that the rotation of the angle of the linearly polarized light should rely only on the magnetic field (created by the current in the current carrying conductor). And it should be made independent of other variables. The interaction length and wavelength are constant. But the temperature is a variable that cannon be made constant. The temperature dependency of Verdet constant has a dramatic effect on the accuracy of the OCS. When there is a change in the temperature, the accuracy of the OCS is lost.

A number of techniques have been proposed to compensate the effect of the temperature dependant Verdet constant on the OCS. One passive compensation technique has been implemented. In this technique $Bi_{12}SiO_{20}$ (BSO) crystal is used as the Faraday sensing element. They used a right and left optical rotary power glasses in required proportions of length to obtain the compensation. As temperature increase one glass will rotate in one direction and the other will rotate in the opposite direction in order to compensate the change in temperature [11]. In this approach due to the left and right

rotary power the resultant Verdet constant is decreased which leads to decreased sensitivity.

Another active approach is to simultaneously measure temperature and magnetic field (produced by the current) in a Faraday effect based current sensor. The technique is based on inter ferometric phase measurement of temperature combined with magnetic-field-induced visibility modulation of the inter ferometric fringes. A paramagnetic FR 5 glass is used as the sensing element and farady-parot configuration is employed [12]. This approach used signal processing techniques to calculate the phase difference which require complex electronics.

The temperature dependence of Verdet constant can also be stabilized by using bi-doped garnet. Bi-doped garnet is a rare metal iron garnet made up of a ferromagnetic substance, of which some portion of the rare metal element is replaced with bismuth. Bi-doped garnet based crystals have fairly linear temperature characteristics between -10 to 80 ^{0}C [13]. So the temperature compensation is directly achieved. In one another technique, it use a dual loop path with no accumulated phase difference in which the light is sent back along nearly the same path in the reverse direction by means of a specially designed quadruple reflection prism [14].

Various other techniques are also used like, to protect the sensor from temperature externally by insulating the whole setup. In another approach permanent magnet is used to provide a DC field component to the sensing element such that the ratio of static and periodic fields is independent of temperature [8, 9]. Some technique proposes that use of a bi-metallic coil to rotate the sensing element mechanically, thus increasing or

decreasing the field component acting on the sensing element as function of temperature [10].

The techniques described above have been able to compensate the temperature dependent Verdet constant. So the accuracy of the OCS has been achieved to some extent. But in the process of compensating they have either sacrificed the sensitively or the dynamic range. The sensitivity of the OCS has been affected due to passive compensation techniques. And techniques require the use of highly complex digital circuits or large amounts of expensive bulk glass sensing materials.

The purpose of study is to make a contribution to the field of OCSs. The aim is to

- Design an OCS that has a good stability, accuracy and has a large dynamic range.
- Find new ways to detect the temperature around the sensor and to determine the effect of temperature on the accurateness of the OCS.
- Propose various ways to compensate the effect of temperature on the accurateness of the OCS.

An innovative active approach to measure both the temperature and the magnetic field (the current in the conductor), by the use of two different frequencies for exciting the coils of the magnetic core has been designed. The current and temperature readings are taken in a controlled environment by the OCS (database mode) and the readings are fed into a database. Now the current and temperature readings from the OCS (sensing mode) are used to look up at the database table, and give the corresponding temperature and current value. A part form the OCS setup, an additional power source operating at a

different frequency and a look up table system is used in this method. Neither a complex digital signal processing system nor extra rare earth bulk glass material is used to achieve the temperature compensation. Finally the effect of the modulating or the excitation frequency on the resultant magnitude of the Digital Signal Processing (DSP) lock in amplifier is observed.

1.3 The Main Objectives of the Study are as Follows:

- To generate magnetic fields of varying frequencies in the air gap of the magnetic core by using the excitation coils of the magnetic core.
- To measure the difference signal at DSP lock in amplifier, that corresponds to the electrical signal produced by the two photodiodes. The change in the intensity of the laser light components is caused by the rotation of the polarization angle which is detected by the two photo diodes. The angle of rotation is proportional to the magnetic field produced by the current in the conductor.
- To apply two distinct frequencies to the coils of the magnetic core, and observe how the resultant magnitude at the DSP lock in amplifier is varying with the change in temperature or current and both. Measure both the current and temperature and propose a method to compensate the change due to the changes in temperature.

- To determine the effect of the modulating (the excitation) frequency on the resultant magnitude of the DSP lock in amplifier, at constant current and temperature.

1.4 The Proposed Setup

The magnetic core has the air gap cut in it. An electromagnet is obtained by passing a current carrying conductor through the center of a core or it is wound around the iron core as a coil. The electromagnet produces the magnetic field proportional to current in the conductor. The sensing element i.e. the crystal bulk glass is place in the air gap between the polarizer (the first Polarization Beam Splitter (PBS)) and analyzer (the second PBS). A linearly polarized light is focused on to the sensor prism, before passing through the PBS (the analyzer) which converts the laser light to a linearly polarized light. Because of the magnetic field the linearly polarized light will rotate an angle of θ due to the Faraday rotation.

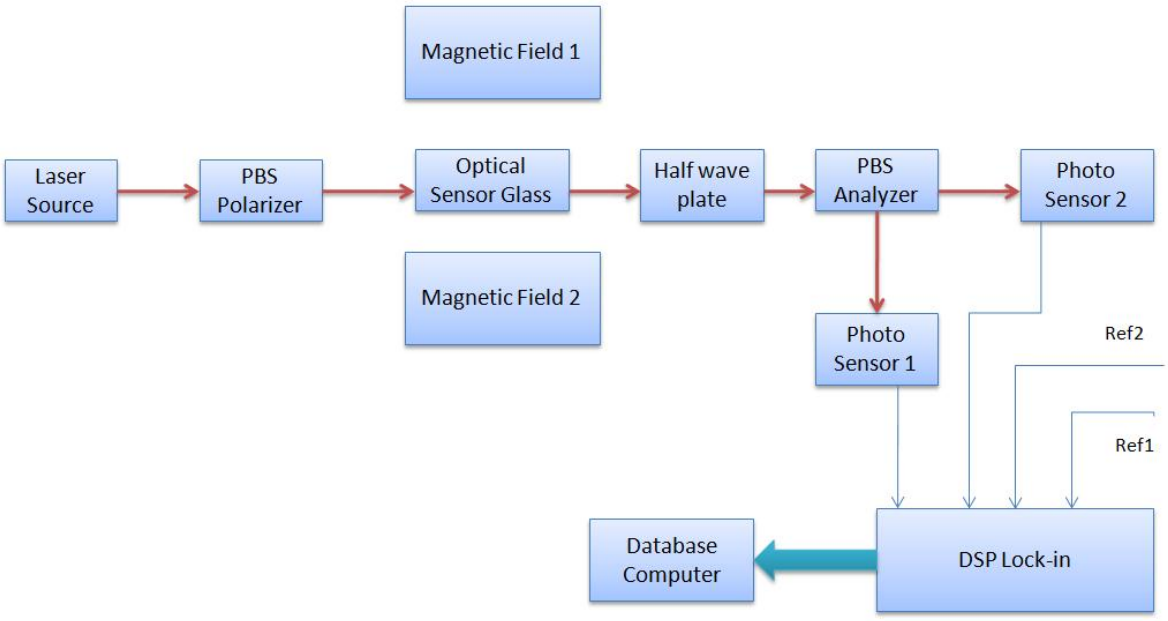

Figure 1: The block diagram of the OCS.

Now the light is reflected back from the crystal and falls on the half wave plate. The half waver plate is used to rotate the polarization of the light by $\pi/4$ (when rotated to 22.5 degrees) so that the polarization of the light is 45 degrees relative to the input polarization at the PBS analyzer. The PBS analyzer will send the horizontal component to the first photo sensor and the other vertical component of the power to the second photo sensor. Then the differential output of the power is calculated at the DSP lock in amplifier. The block diagram is in figure 1. As the output depends on the polarization rotation which is dependent on the magnetic field generated by the current carrying conductor, the change in current can be sensed. The reference signal to the DSP lock in amplifier is taken from the line voltage through a step down transformer. The current readings and their corresponding output at the DSP lock in amplifier are tabulated for different temperatures. Now the other reference to the DSP lock in is taken from the

function generator, which generated the current in the secondary coil. Here the current in the coil is constant and the change in the temperature alone caused the change in the output of the DSP lock in amplifier. So by using two distinct frequencies to generate the magnetic field in the air gap, both the current and temperature can be detected. By using a look up table the changes in the temperature are compensated.

1.5 Scope of the Study

The study focuses on possible use of two power sources of distinct frequencies to excite the coils of magnetic core, to produce distinct magnetic fields. These fields modulate the laser beam, and using the reference signal from the power sources, we measure the difference signal at the DSP lock in amplifier. One frequency of power will be used to measure the current in the power line, while the other frequency of power is used to detect the temperature changes. This study is limited to find ways to detect both the temperature and current, and propose ways to compensate the temperature changes in the difference value of the resultant at DSP lock in amplifier. The temperature compensation techniques are just proposed, but they are not design or fabricated.

CHAPTER 2

BACKGROUND

2.1 Faraday Effect

Michael Faraday in 1845 discovered that the manner in which light propagated through a material medium could be influenced by the application of an external magnetic field. He discovered that the plane of vibration is rotated when the light path and the direction of the applied magnetic field are parallel. The Faraday effect occurs in many solids, liquids, and gases. The magnitude of the rotation depends upon the strength of the magnetic field, the nature of the transmitting substance, and Verdet constant, which is a property of the transmitting substance, its temperature, and the frequency of the light. The direction of rotation is the same as the direction of current flow in the wire of the electromagnet, and therefore if the same beam of light is reflected back and forth through the medium, its rotation is increased each time [17]. The relation betweenθ, B, L and V is by the equation

$$\theta = BLV \qquad \ldots (1)$$

The polarization plane of the light, which is defined as the plane containing the electric field vector of the light to the direction of light propagation, is rotated by an angle θ. Where V the Verdant constant of the prism glass material, B is is the magnetic flux density and L is the optical path length along the magnetic field. The plane of vibration,

when V is positive, rotates in the same direction as the current in the coil, regardless of the beam's propagation direction along its axis. The effect can, accordingly, be amplified by reflecting the light back and forth a few times through the sample. [16]

2.2 Verdet Constant

The Verdet constant is an optical constant that describes the strength of the Faraday effect for a particular material. The Verdet constant is wavelength dependent and is proportional to λ. The following equation expresses the Verdet constant's dependency on the wave length. [15]

$$V = -\frac{e\,\lambda}{2\,m\,c}\left(\frac{dn}{d\lambda}\right)$$

$\frac{dn}{d\lambda}$ is the dispersion of intrinsic index.

λ is the wave length.

c the speed of light.

e, m are the charge and mass of the electron.

The Verdet constant is also dependent on temperature, and it is discussed in section 3.2.2

2.3 Polarization

Light waves are transverse in nature. Transverse waves consist of disturbances that are at right angles to the direction of propagation. The vibrating electric vector associated with each wave is perpendicular to the direction of propagation. A beam of

non polarized light consists of waves moving in the same direction with their electric vectors pointed in random orientations about the axis of propagation. Randomly polarized light can be seen in figure 2.1. A Linearly or Plane polarized light consists of waves in which the direction of vibration is the same for all waves as in figure 2.2. In circular polarization the electric vector rotates about the direction of propagation as the wave progresses as in figure 2.3. Light may be polarized by reflection or by passing it through filters, such as certain crystals, that transmit vibration in one plane but not in others. [18]

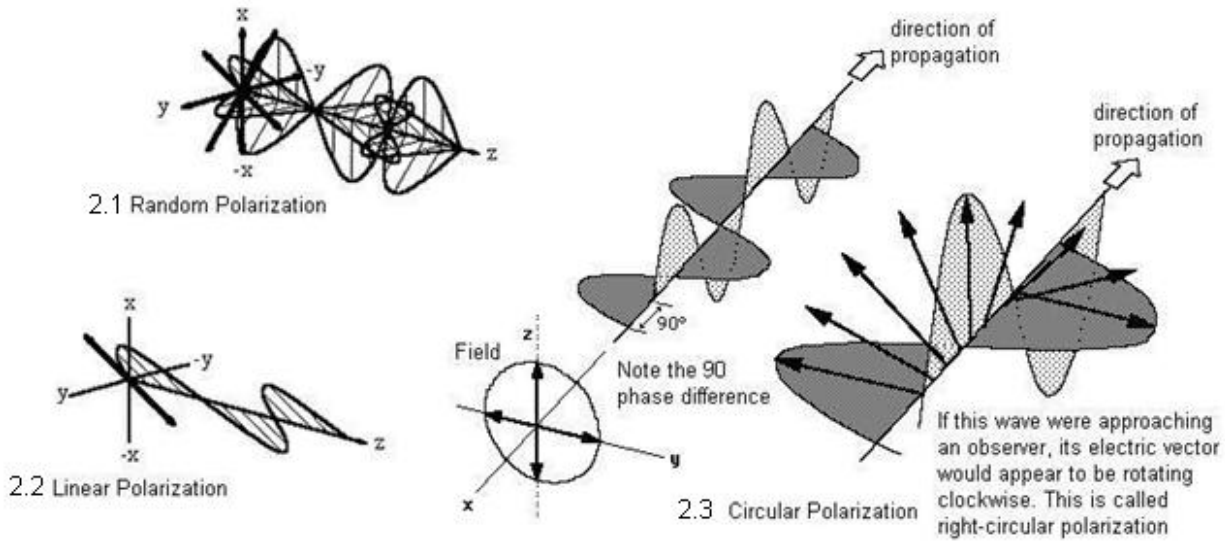

Figure 2: Random, linear and circular polarization of light [30] [31].

2.4 The Right Angle Prism and the Porro Prism

The Porro prism is physically the same as the right angle prism but is used in a different orientation. As shown in figure 3 after two total internal reflections, the beam is

deviated by 180^{o}. The beam enters right handed, and it leaves right handed. [22]. The rotation of the plane of polarization is proportional to the intensity of the component of the magnetic field in the direction of propagation if the laser beam. The length between the incident and reflected light beams in figure 3 is the interaction length that will undergo Faraday rotation.

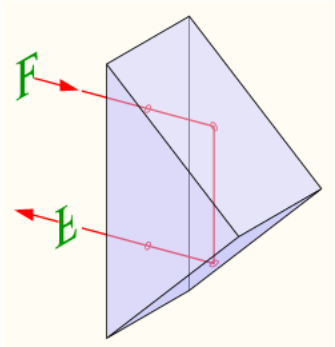

Figure 3: The Porro prism [32].

2.5 Total Internal Reflection

The relation between the angle of refraction and incidence θ_1 and θ_2 in figure 4, at a planar boundary between two media of refractive indices n1 and n2 is governed by Snell's law. The law says that the ratio of the sines of the angles of incidence and of refraction is a constant that depends on the media.

The refracted ray lies in the plane of incidence; the angle of refraction θ_2 is related to the angle of incident θ_1 [21]

$n_2 \sin \theta_2 = n_1 \sin \theta_1$

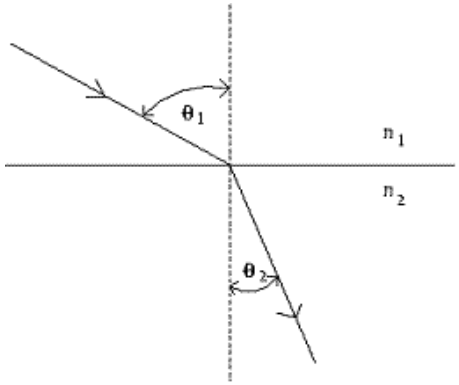

Figure 4: Law of refraction [29].

For internal reflection (n1 > n2) the angle of refraction is greater than the angle of incidence $\theta_2 > \theta_1$. And when θ_1 is greater than θc, the incident light will not refracted, instead it will be totally reflected back into the same medium. θc is the critical angle given by

$$\theta c = \sin^{-1}(n_2 / n_1).$$

2.6 Polarization Rotators

A polarization rotator rotates the plane of polarization of a linearly polarized light by a fixed angle, maintaining its linearly polarized nature. Optically active media and materials exhibiting the Faraday effect act as polarization rotators. The sensor glass is actually a polarization rotator. The intensity of light is controlled (modulated), by the angle of rotation which is controlled by external means (by varying magnetic flux density applied to a Faraday rotator). [20]

2.7 Half Wave Plate

A half wave plate is a retardation plate that introduces a relative phase difference of π radians or 180 degrees between the polarization planes. The retardation plate introduces a lag of some predetermined value from the other polarization plane.

2.8 Polarizer and Polarization Beam Splitters

A polarizer is a device that transmits the component of the electrical field in the direction of its transmission axis and blocks the orthogonal component. This is achieved by selective absorption and selective reflection. While a polarization beams splitters split randomly polarized beams into two orthogonally linearly polarized components. In figure 5, the S and P polarized light are incident on to a polarization beam splitter (PBS). The S-polarized light is reflected at a 90 degree angle while P-polarized light is transmitted.

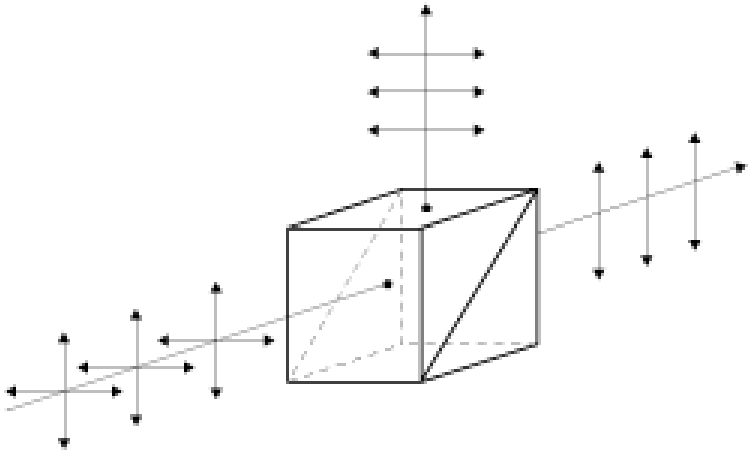

Figure 5: Polarization beam splitting of light [33].

2.9 Laser

Light amplification by stimulated emission of radiation. Laser light is usually spatially coherent, which means that the light either is emitted in a narrow, low-divergence beam, or can be converted into one with the help of optical components such as lenses. The principal light sources used for fiber optic communication applications are hetero junction – structured semiconductor laser diodes and light emitting diodes (LEDs). A hetero junction consists of two adjoining semiconductor materials with different band-gap energies. These devices are suitable for fiber transmission systems because they have adequate output power for a wide range of applications, their optical power output can be directly modulated by varying the input current to the device, they have a high efficiency, and their dimensional characteristics are compatible with those of the optical fiber. [19]

CHAPTER 3

METHODOLOGY

3.1 The Experimental Setup

The Faraday effect is basic principal used in designing an optical current sensor (OCS). The changing electrical current flowing through the conductor of the magnetic core concentrator generates a magnetic field across the air gap of the core, where the sensor glass is placed. The linearly polarized laser light experiences a shift in the angle of the plane of polarization, when passed through the sensor prism in the magnetic field. The angle of rotation is a function of magnetic field in the air gap, the temperature and Verdet constant of the prism glass. The magnetic field produced by an electromagnet, is proportional to the product of the current through the electromagnet and the number of turns of the wire around the coil. Because of the rotation in the angle of the plane of polarization, the vertical and horizontal components of the linearly polarized light changes. The vertical and horizontal components are detected by a difference method. The laser light after passing through a polarization beam splitter (PBS) in figure 6, coming from the prism and half wave plate is sensed by two photo diodes. The photo diodes convert the light signal into an electrical signal. This signal is fed to a digital signal processing (DSP) lock in amplifier where the resultant difference signal is detected, at the frequency of the reference signal fed into the DSP lock in.

The current and temperature are measured with the help of a duel frequency method. To detect the line current in the conductor or coil, a small signal from the line current is fed to the reference of the lock in. To detect the temperature, the coil is excited with an electrical signal of a frequency different from the line frequency, and a small sample of this frequency signal is applied to the reference of the lock in. The temperature and current readings obtained are look up at the database value to give the actual output. Controlled environment is maintained to record the values in the database that maps the current and temperature magnitude values at the DSP lock in amplifier, to the actual temperature and current. By this method we can achieve better compensation to the temperature changes, with a large dynamic range and better sensitivity. A detailed explanation of the experimental setup is given in the subsequent sections.

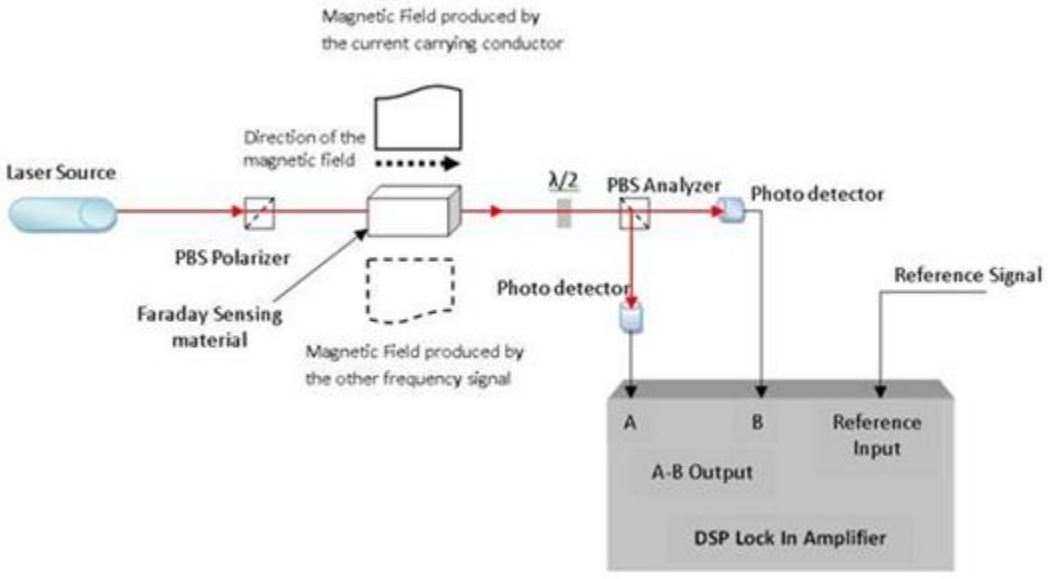

Figure 6: The schematic experimental setup.

3.2 The Optic Current Sensor Design

The setup of the OCS design has three important steps.

- The magnetic field setup
- The sensor element
- The analysis method

3.2.1 The Magnetic Field Setup

A magnetic field is generated by the current flowing through a current carrying conductor, because of the electromagnetic effect. But this is distributed in all directions. A field concentrator is used to focus the magnetic field around the conductor into a small area where the sensor glass is place.

A square shaped current transformer (CT) from Flex-Core (multi ratio transformer Model 331-200) [28] is used initially. An air gap of 14 mm is cut in, to place the sensor glass. By exciting the coils with a variac magnetic field is produced in the air gap. But when the current in the coil reached higher orders the arms of the core started to vibrate. So we thought of using powered magnetic core. While cutting the air gap in to the circular core, it broke off. So the laminated circular iron core with the air gap cut in it is used. The Toroid T02091XX1 for electro core Inc is used. Either a wire is wound around the iron core 360 times or a high tension electric cable is passed through the center of the

core to convert the iron core into an electromagnet that generates the magnetic field by the flow of current. Figure 7 shows the actual 360 turn wire setup. The 360 turn wire is excited by a variac that controls the current flow, to produce the magnetic field in the air gap of the circular core.

A welding cable or a ¾ inch high tension cable is also used in closed loop as the current carrying conductor. The current in the conductor loop is generated by placing either one or three of the current transformer. The Model 195-202 metering class CT is used with current ratio of 2000:5 from Flex-Core [34]. These CTs are actually designed to calculate the current flowing through the conductor by detecting the magnetic field, but they are being used in the reverse mode. The current is applied to the CTs and they produce the magnetic field; and this field will in turn produce the current in the conductor loop that passed through the CTs. The CTs are connected in parallel to the variac that control the current in the loop. Figure 25 shows the actual current loop setup. Either a single or a double loop setup is used in which the loop runs through the circular iron core that generates the magnetic field in the air gap, one or three metering class CTs that generate current, and another metering class CT that acts as an ammeter (normal mode of the CT) in the loop.

The hall probe of the DSP 455 gauss meter is placed in the air gap of the core to measure the magnetic field produced.

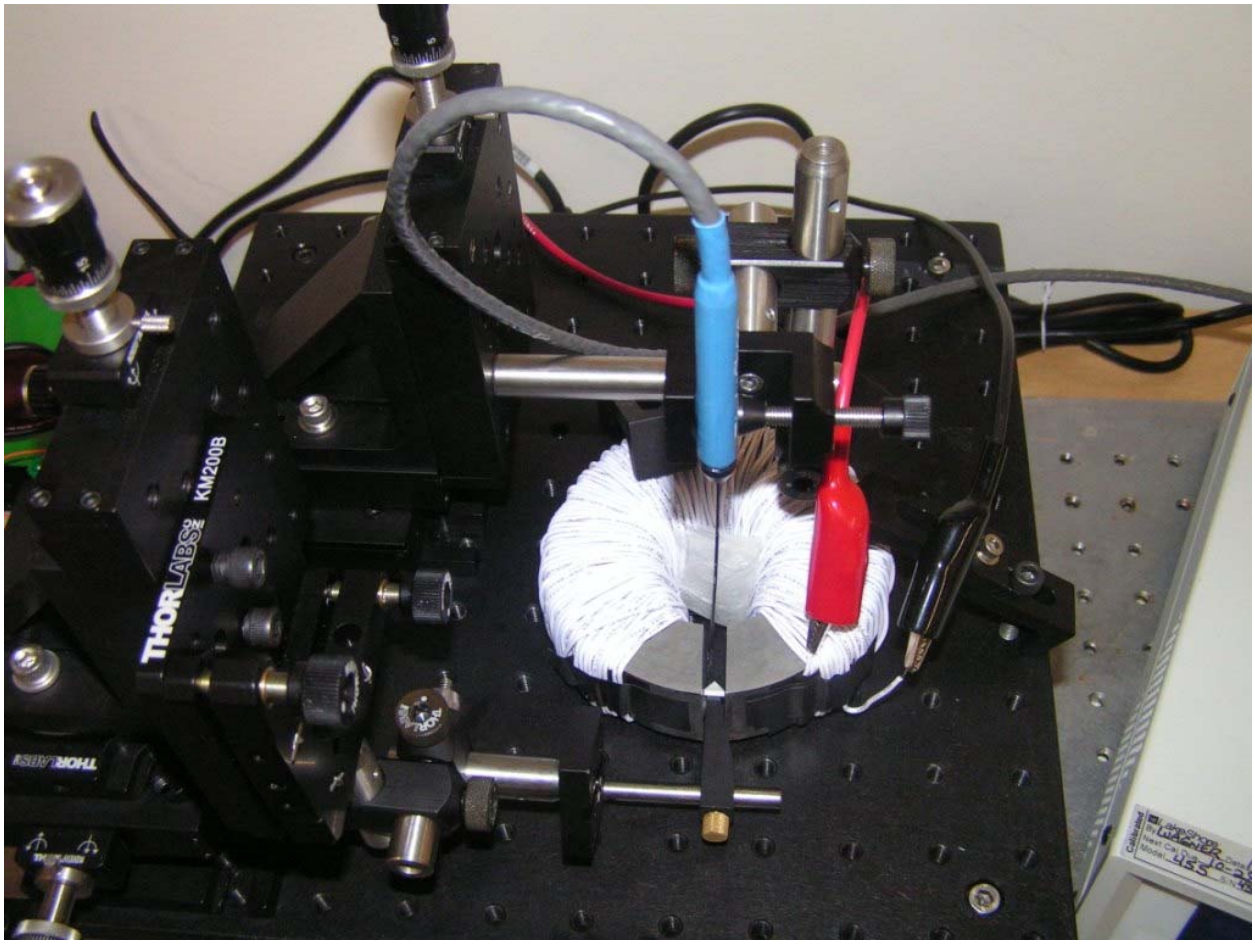

Figure 7: The experimental setup of the circular magnetic core with wire wound around it.

3.2.2 The Sensing Element

Optical method is used to measure the magnetic field produced by the current in the air gap. A linearly polarized light is propagated through the SF57 sensor glass prism. As a result of the Faraday effect, the polarization plane of the light, which is defined as the plane containing the electric field vector of the light to the direction of light

propagation, is rotated by an angle θ because of the magnetic field. The rotation of the plane of polarization is proportional to the intensity of the component of the magnetic field in the direction of propagation of the laser beam.

The mathematical approach to find magnetic flux density for this experimental setup is explained below initially. And then the mathematical approach for the rotation of the polarization angle is discussed.

The magnetic circuit concepts are used, which are analogous to those used to analyze electrical circuits that help us to analyze transformers and generators that contain coils wound on iron cores.

The magneto motive force (mmf) of an n turn current carrying coil is given by $F = ni$.

Magneto motive force is analogous to source voltage. The reluctance of a path is given by

$$R = \frac{l}{\mu A}$$

Where l is the length of the path (in the direction of the magnetic flux), A is the cross sectional area and μ is the permeability of the material.

Magnetic flux Ø in a magnetic circuit is analogous to the current in an electrical circuit.

Magnetic flux, reluctance, and magneto motive force are related by

$F = R\emptyset$ which is the counter part of Ohms law $V = iR$

So from the magnetic circuit equations we have

$F = nI$ and $F = R\phi$

So $nI = R\phi = BAR$

$nI = \mu HAR_{total}$

As the magnetic flux is given by $\phi = BA$

And magnetic flux density $B = \mu H$

Where H is the magnetic field intensity, and μ is the magnetic permeability

With the aid of the above equations we derive the magnetic flux density for a circular core, with n number of turns round the core. The various physical properties and their notations are given below. In Figure 8 some of notations have been labeled.

R_{core}^{mc}	Reluctance of the magnetic core
R_{gap}^{air}	Reluctance of the air gap
L_{core}	Length of the magnetic core
L_{gap}^{air}	Length of the air gap
$\mu^{mc}(\mu_r^{mc})$	Permeability (relative) of the magnetic core
$\mu^{hs}(\mu_r^{hs})$	Permeability (relative) of the Hall sensor
A_{cs}^{mc}	Cross sectional area of the magnetic core
A_{gap}^{air}	Cross sectional area of the air gap
$L_{r,ct,cw}^{mc}$	Length of the magnetic core (core radius, core thickness and core width)
I	Current flowing through the coil.

Reluctance of the core $R = l/\mu A$

$$R_{core}^{mc} = \frac{L_{core} - L_{gap}^{air}}{\mu^{mc} A_{cs}^{mc}}$$

Reluctance of the air gap

$$R_{gap}^{air} = \frac{L_{gap}^{air}}{\mu^{hs} A_{gap}^{air}} = \frac{L_{gap}^{air}}{\mu^{hs} A_{gap}^{air}} = \frac{L_{gap}^{air}}{\mu_o \mu_r^{hs} (L_{ct}^{mc} + L_{gap}^{air})(L_{cw}^{mc} + L_{gap}^{air})}$$

As magnetic circuit equations are given by

$$\text{We have} \qquad nI = \mu H A R_{total}$$

$$B = nI / AR_{total}$$

$$B = \frac{\mu_0 nI}{\mu_r^{hs} A_{gap}^{air} (R_{core}^{mc} + R_{gap}^{air})}$$

$$B = \frac{\mu_0 nI}{L_{core} \frac{\mu_r^{hs}}{\mu_r^{mc}} \frac{A_{gap}^{air}}{A_{cs}^{mc}} + L_{gap}^{air} - L_{gap}^{air} \left(\frac{\mu_r^{hs}}{\mu_r^{mc}} \frac{A_{gap}^{air}}{A_{cs}^{mc}} \right)} \qquad \ldots (2)$$

From equation (1) the angle of rotation of the plane of polarization and its relation to the magnetic field, Verdet constant, interaction length is given by

$$\theta = \frac{n I V L}{\mu_0 \mu_r^{hs} A_{gap}^{air} \left(\frac{L_{core} - L_{gap}^{air}}{\mu^{mc} A_{cs}^{mc}} + \frac{L_{gap}^{air}}{\mu_0 \mu_r^{hs} A_{gap}^{air}} \right)} \quad \ldots (3)$$

The SF57 bulk glass is used as the sensing material (glass sensor). SF57 is selected because of its high Verdet constant. From the above equation one can observe that a high Verdet constant will yield in a higher angle of rotation, which in turn will increase the sensitivity. Here is a table of different glasses and their Verdet constants. Glasses are at 20 °C and 589.3 nm.

Table 1: Verdet constant of various glasses [34].

Glass	r/(10^{-2} min A^{-1})
Hard crown (nD = 1.519)	2.4
Dense Barium crown (nD = 1.612)	2.4
Light flint (nD = 1.579)	3.9
Dense flint (nD = 1.623)	4.85
Extra dense flint (nD = 1.700)	6.55
SF 57 (nD = 1.846)	10.3

The properties of various glasses can be found the datasheets provide by Schott [23]. As mention above, the Verdet constant changes with wavelength. The Verdet constant also changes with temperature. The change in the temperature induces an angle shift in the polarization plane. Thus the magnitude or the output value at the DSP lock in value varies. Normally with an increase in the temperature, the resultant magnitude at the DSP lock in amplifier decreases. The relation between the angle of rotation of the polarization plane (θ), the magnetic field (B) across the air gap (L_{gap}^{air}), the Verdet constant (V), and the temperature (T) is given by the equation [35]

$$\frac{d\theta}{\theta.dT} = \frac{dB}{B.dL_{gap}^{air}}\frac{dL_{gap}^{air}}{dT} + \frac{dL_{gap}^{air}}{L_{gap}^{air}.dT} + \frac{dV}{V.dT}$$

For SF57 glass the Verdet constant varies from 70 rad/T.m at 400 nm to 20 rad/T.m at 680 nm. For making a high sensitive and accurate OCS, the change in θ must be only be contributed by a change in the magnetic field, but not the temperature.

3.2.3 The Analysis Method

The rotation in the angle of the polarization plane has to be detected, which corresponds to the magnetic field produced by the current carrying conductor. The difference method is used to detect the angular shift in the polarization plane of the light. The shift in the rotation of polarization plane affects both the vertical and horizontal components and by measuring the intensity of both the components, we can detect the change in the angle of polarization plane. As depicted in the figure 8, the vertical and horizontal components are obtained, when the laser coming from the sensor prism, after passing through the half wave ($\lambda/2$) plate, hits the analyzer PBS. The half wave plate has been rotated and fixed at 22.5 degree angle, which imparts a 45 degree shift between the incident and transmitted laser beam's plane of polarization. The light signal of each component is converted into electrical signal by the two SM05PD1A photo diodes placed after the PBS (analyzer) in figure 8. The electrical signal for each photo diode is connected to the DSP lock in amplifier, where the difference between the two components is calculated and is being displayed as the resultant magnitude. The DSP lock in only measures only the signals that match the reference frequency

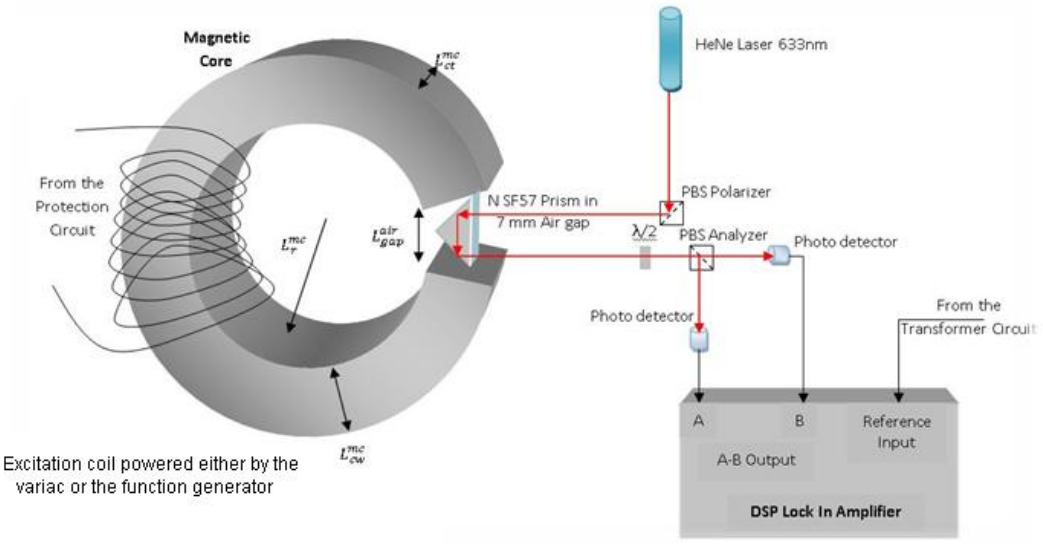

The mathematical approach to the difference method is described below. Let α be the angle between the transmission axes of the polarizer and the analyzer, then the laser light power is given by

$$P_{out} = P_{in} (\cos\alpha)^2$$

$$P_{out} = \frac{1}{2} P_{in}(1 + \cos(2\alpha))$$

Typically the angle α is adjusted to be $\pi/4$. The 45 degree angle is achieved by using the half wave plate. The half wave plate is fixed at 22.5 degrees, to impart a 45 degree angular shift between the polarizer and the analyzer. In the experimental setup we have placed the half wave plate between the SF57 sensor prism and the analyzer PBS show in figure 8. With no field applied, the optical power input to the photo detector is

then only half the input power. When the rotation angle θ is small, the change in photo detector output is practically a linear function of the field. In the above equation if we substitute, $\alpha = \pi/4 + \theta$ and the output of the first and the second photo sensor will be

$$P_{out1}(t) = \frac{1}{2} P_{in}(1 - \sin(2\theta(t)))$$

$$P_{out2}(t) = \frac{1}{2} P_{in}(1 + \sin(2\theta(t)))$$

Comparing the difference of the two polarization components to their sum gives

$$\frac{P_{out2} - P_{out1}}{P_{out2} + P_{out1}} = \sin(2\theta) \qquad \ldots (4)$$

The current under detection can be expressed as the follows using the (2), (3) and (4) equations

$$I = \left. \mu_0 \, \mu_r^{hs} \, A_{gap}^{air} \left(\frac{L_{core} - L_{gap}^{air}}{\mu^{mc} \, A_{cs}^{mc}} + \frac{L_{gap}^{air}}{\mu_o \, \mu_r^{hs} \, A_{gap}^{air}} \right) 2 \sin^{-1} \left(\frac{P_{out2} - P_{out1}}{P_{out2} + P_{out1}} \right) \right/ n \, V \, L$$

The current in the coil can be measured by this magneto optical method. By sensing the optical power of the vertical and horizontal laser beam components, we can detect the current in the coil; by referring to the resultant magnitude of the DSP lock in amplifier. But from the above equation, the current readings are also affected by Verdet constant which is temperature dependent. To compensate the temperature changes, an innovative duel frequency method has been implemented.

In this method we use two different frequencies for exciting the coils of the circular core. The main purpose of an OCS is to detect the current in a conductor. To overcome the temperature dependency problem, two coils are used, excited each of them with two different power sources operating at two different frequencies. One of the coils is connected to the power source (line power) in which the line current is to be detected. This generates a magnetic field in the air gap of the circular core with a frequency same as the operating line frequency. The reference signal to the DSP lock in amplifier is given from the step down transformer connected to the line current. The DSP lock in detects only the signal that are modulated at line frequencies. First the temperature is kept constant and the current reading are taken for a range of values in steps. Then the temperature is incremented and the current readings are taken for the range of values in steps. The entire range of current and temperature database is obtained by placing the OCS in a controlled environment. The readings of the DSP lock in amplifier (step down transformer as reference) are tabulated, with the current in the coil on horizontal rows, and temperature on the vertical columns. The data base maps the readings obtained on the DSP lock in amplifier reference magnitude to the actual current and temperature value. The readings thus obtained are affected by both the current and temperature.

As we know that the change in the temperature will change the polarization plane angle. To detect the temperature around the sensor, the secondary coil is excited by a different source (function generator), which will excite the coil at a constant current value, with a frequency different from the line frequency. So this will create another but constant magnetic field across the air gap with a different frequency. The laser light will

carry both the modulated signal. As the signal from the sync output of the function generator is applied as the DSP reference signal, only the signals at the frequency of the function generator will be detected. As the current in the secondary coil is kept constant, any change in the magnitude of the DSP lock in magnitude (reference fed from function generator) value reflects a change in the temperature. Keeping the current constant, the temperature is varied in steps, and these values are entered into a data base that maps the actual temperature.

Now both the values from the current sensor and temperature sensor are used to look up at the data base table. The temperature sensor magnitude value acts as an index to the select the particular row that the current values are to be matched, and displayed. So by this active method we could effectively compensate the effect of changes in the temperature on the current reading. In this the range and the sensitivity of the OCS are not compromised. Proposed lookup table method to compensate the temperature dependency on the outcome of the current readings of the OCS is depicted in figure 10. The temperature sensor readings act as an input to select the particular row from the column table. And the current sensor readings act as an input to select the particular column from the rows of the data base.

An analog compensation technique can also be developed, by studying the mathematical behavior. One can compensate the change to temperature for the OCS by using some kind of analog circuit. But to design the analog compensation circuit, we need to understand how the temperature has its effect on the current readings (power form variac), and how the temperature readings are changing with the change in the

temperature (function generator source) which has been performed using the dual frequency method.

Data from the temperature sensor

Data from the current sensor, with current and temperature varying

TEMP	Current measured at different temperatures at the DSP lock in											
2nd coil	Current	10A	20A	30A	40A	50A	60A	70A	....	500A	....	1000A	2000A
400	DSP 01	100	105	110	115	120	125	130	....	400	....	840	1505
395	DSP 02	90	100	105	110	115	120	125	....	390	....	830	1500
390	DSP 03	80	90	100	105	110	115	120	....	380	....	825	1495
385	DSP 04	70	80	90	100	105	110	115	....	370	....	820	1490
...	....	....	....	....	....	....	....	....	....	....	....	....	....
260	DSP 40	40	50	60	70	80	90	100	....	300	....	500	1000
255	DSP 41	30	40	50	60	70	80	90	....	295	....	495	995
....	....	....	....	....	....	....	....	....	....	....	....	....	....
100	DSP 80	1	10	20	30	40	50	60	....	200	....	410	820

Proposed lookup table method to compensate the temperature changes

Figure 9: Lookup table method.

The snapshot of the actual experimental setup with the laser beam, sensor glass placed in the air gap of iron core wound with the coil around it, the hall probe, PBS's, half wave plate and the photo diodes are shown in the figure 10 below.

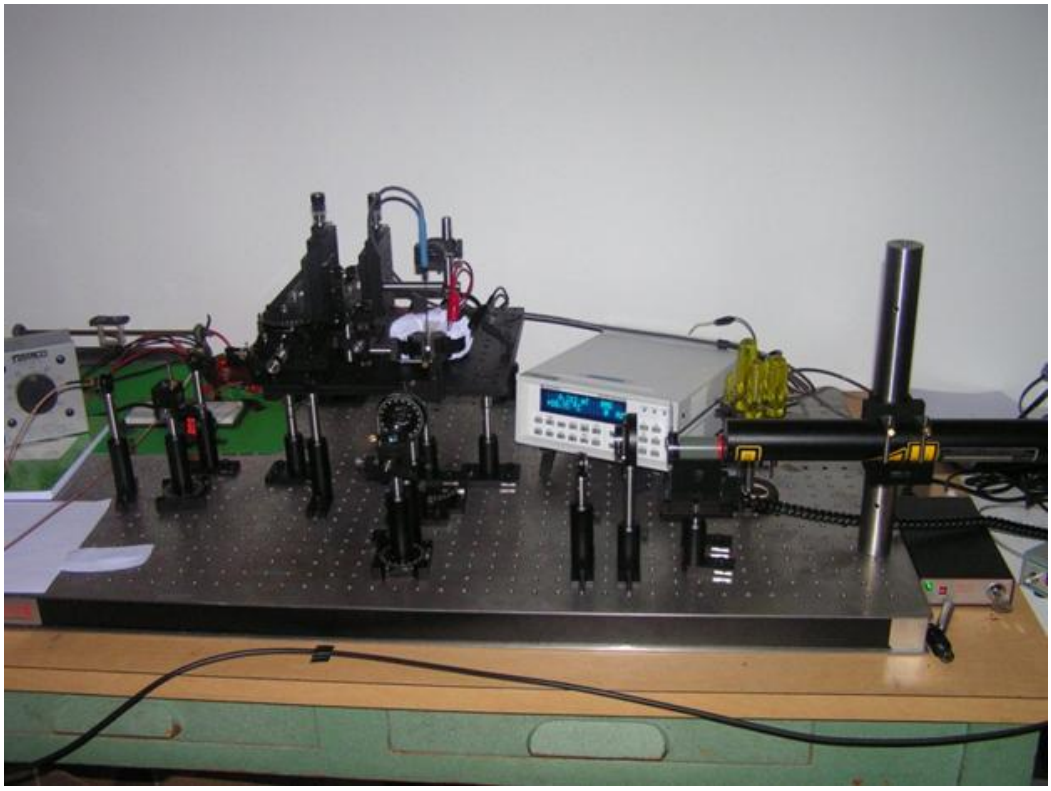

Figure 10: The experimental setup of the OCS in the optics lab.

CHAPTER 4

INSTRUMENTATION

Before starting the experiments, following things other than reading research papers had to be learnt and completed in order to have a sufficient base to conduct my experiments and proceed towards my thesis topics.

Following is the list of things and software's learnt,

4.1 Digital Signal Processing (DSP) Lock in Amplifier

DSP lock in amplifier (SR 830) from Stanford research systems is used to detect the difference signal form the photo detector. The reference signal to the DSP lock in is fed either from the function generator or the line power source, through a step down transformer. The corresponding change in the laser light's polarization angle due the magnetic field (caused by current in the power line), is converted to electrical form by the photodiode. But the signal from the photodiode is very small, and in order detect a change in the signal strength a DSP lock in amplifier is required. Here the signal is amplified and converted to digital signal, which is then displayed on the front panel.

Lock-in amplifiers are used to detect and measure very small alternating currents (AC) signals, down to a few nanovolts. Accurate measurements can be made even when the small signal is obscured by noise sources many thousands of times larger. Lock-in amplifiers use a technique known as phase-sensitive detection to single out the

component of the signal at a specific reference frequency and phase. Noise signals at frequencies other than the reference frequency are rejected and do not affect the measurement.

Lock-in measurements require a frequency reference. The excitation frequency fed to the core is used as the reference to the lock in. In the figure 11 below, the reference signal is a square wave at frequency ωr. This is the sync output from a function generator. If the sine output from the function generator is used to excite the experiment, the response might be the signal waveform shown below. The signal is Vsig sin(ωr + θsig)

Where Vsig is the signal amplitude.

The SR830 generates its own sine wave, shown as the lock-in reference below. The lock-in reference is V_L ($\omega_L t + \theta_{ref}$). The SR830 amplifies the signal and then multiplies it by the lock-in reference using a phase-sensitive detector or multiplier. The output of the phase sensitive detector PSD is simply the product of two sine waves.

$V_{PSD} = V_{sig} V_L \sin(\omega_L t + \theta_{sig}) \sin(\omega_L t + \theta_{ref})$

The PSD output is two AC signals, one at the difference frequency ($\omega_r - \omega_L$) and the other at the sum frequency ($\boldsymbol{\omega}_r + \boldsymbol{\omega}_L$). If the PSD output is passed through a low pass filter, the AC signals are removed. In the general case, there will be nothing. However, if ω_r equals ω_L, the difference frequency component will be a direct current (DC) signal. In this case, the filtered PSD output will be

$V_{PSD} = 1/2\ V_{sig} V_L \cos(\theta_{sig} - \theta_{ref})$

Which is a very nice signal - it is a DC signal proportional to the signal amplitude [24]

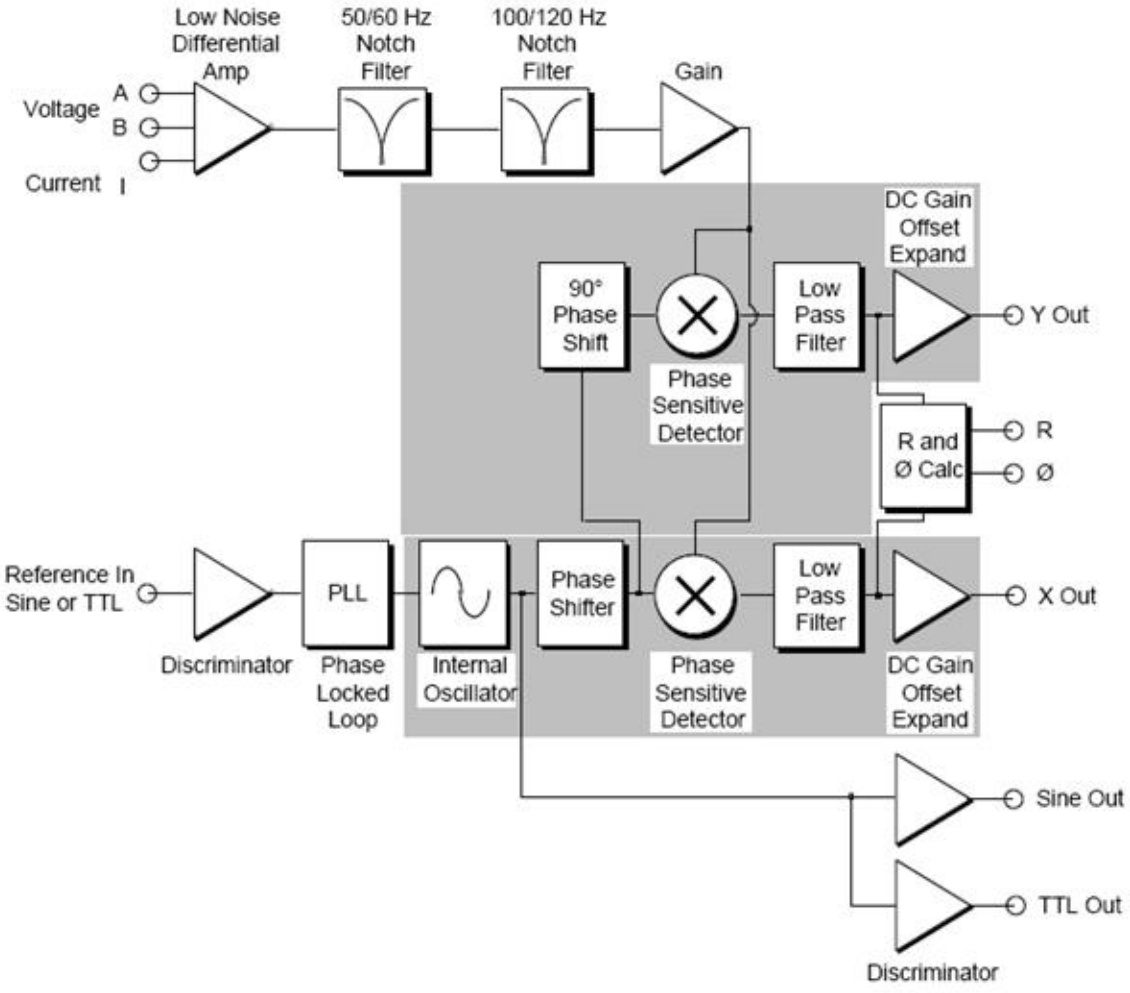

Figure 11: SR830 Block diagram [24].

4.2 Lakeshore DSP Gauss Meter 455

The DSP gauss meter 455 from Lakeshore Inc. is used to measure the magnetic field produced in the air gap. The Model 455 digital signal processing (DSP) gauss meter combines the technical advantages of DSP technology with many advanced features. DSP technology gives accurate, stable, and repeatable field measurements. Advanced features including DC to 20 kHz AC frequency range, peak field detection to 50 μs pulse widths,

DC accuracy of 0.075%, and up to 5¾ digits of display resolution make the model 455 ideal for our research applications. It can measure magnetic fields ranging from 35 mG to 350 kG. Model 455 uses a standard Lakeshore Hall probe.[25]

The model 455 offers a wide range of features, with enhance the usability and convenience of the gauss meter. It has Auto range, Auto probe zero to make the present magnetic field to zero and take relative measurements, and can display the magnetic filed in various units and has Max/Min hold features for convenience. The probe is not only capable of measuring the magnetic field, but also the temperature and frequency of the magnetic field.

Figure 12: The front panel of the gauss meter [25].

4.3 SR540 Chopper

The model SR540 optical chopper is used. It is used to square-wave modulate the intensity of optical signals. The unit can chop light sources at rates from 4 Hz to 3.7 kHz. Versatile, low jitter reference outputs provide the synchronizing signals required for several operating modes line, single or dual beam; sum & difference frequency; and synthesized chopping to 20 kHz. The schematic setup of the chopper wheel is shown in the figure. [26]

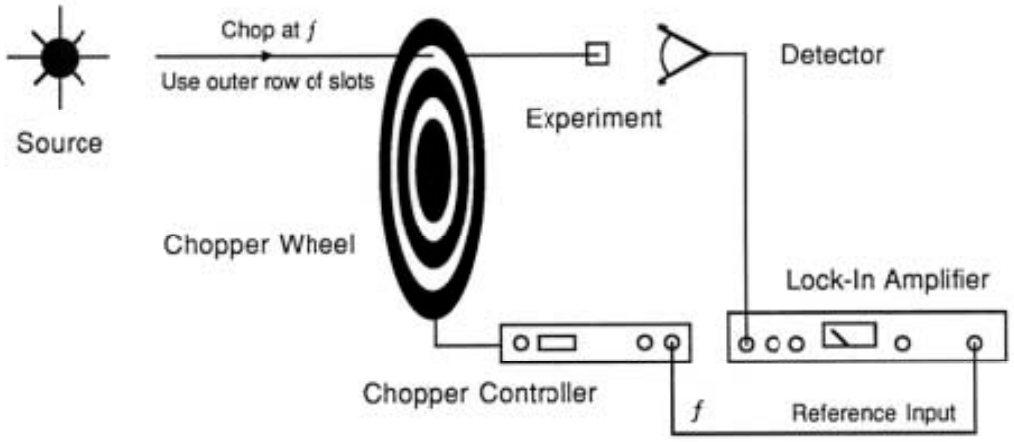

Figure 13: Schematic diagram of the chopper [26].

4.4 33120A Function Generator

The Agilent technologies 33120A is a high-performance 15 MHz synthesized function generator with built-in arbitrary waveform capability. It can generate a wide verity of frequencies and waveforms at voltage level form 0V to 10V. The function generator is use to give the reference input to the DSP lock in, to energize the coil of the

magnetic core, to produce magnetic field for the modulation of the laser light, by producing different magnetic files at different frequencies.

4.5 Photo Diodes

SM05PD1A series of photodiodes are employed from Thorlabs. It consists of InGaAs, Ge, Si, or GaP photodiodes. The electrical output of the sensor is through a standard sub miniature version A (SMA) connector Bayonet Neill Concelman (BNC) connector mounted directly to the housing for quick connection to the measuring circuit. These photodiodes are used to convert the light energy (intensity) incident on the sensor surface to its corresponding electrical signal.

4.6 Photo Meter

Photo meter (PM) is used to initially align the linearly polarized laser beam, so that maximum energy is directed towards the prism after coming out through the PBS. The PM30 series of power meter from Thorlabs are used. The high sensitivity, analog, optical power meters gives analog and digital laser power or other optical power measurements, with detectable signals of 5 nW to 1 W at wavelength ranges of 400 to 1100 nm. With a fast analog display and a complementary 4-digit digital screen, these units are ideal for the fine adjustment of optical setups (free space and fiber optic power measurements) and lasers cavities.

4.7 Magnetic Core

The Split core CT is used to produce the magnetic field from the current. The one we have used is form Flex-Core, Model 331-100. The circular toroid iron core is also used, to produce the magnetic field. The one we have used is from Electro-Core Toroid T02091XX1.

4.8 Matlab Simulation

The experimental setup is simulated, in the Matlab by using the various equations that are derived for our experimental setup. The program is used to know the effect of different parameter on the polarization shift.

4.9 The SF57 Bulk Glass

The SF57 bulk glass right angled prism from Casix is used as the sensing element.

4.10 The Polarization Beam Splitters

The PBS that are employed in our experiment are from the Dayoptics. Its wavelength is 633 nm and its dimensions are 6.35*6.35*6.35.

4.11 Laser Source

The laser source used is a high power HRP050 from Thorlabs. It is a red polarized He-Ne laser, with a wave length of 632.8 nm, and with power outputs up to 5.0 mW. The entire experiment is mounted on Thorlabs optics table located at the optics lab, Discovery Park, UNT.

CHAPTER 5

RESULTS

5.1 Matlab Simulation

Initially the experimental setup is simulated using Matlab software for expecting the outcome. The range, linearity and sensitivity of the setup have been estimated using the simulation. The mathematical equation (3) derived for the current flowing in the conductor is used. The physical properties of the core, prism, the excitation current in the coil and other experimental conditions are substituted into the equation. The program displays the graphs of results simulated, with the magnetic field produced on the vertical axis and the current applied on the horizontal axis. The simulated program has been preformed for various conditions, like with and without sensor. The graphs displayed by the program have exhibited a linear relationship between the current and the magnetic field. The outcome of the program has shown that the setup exhibits a large dynamic range of up to 1500 A. The graphs that have been obtained by the program are attached [Figure 35]. The matlab program that is used to simulate the experimental setup is attached in [Matlab code].

5.2 Using a Square Shaped Magnetic Core, to Produce the Magnetic Field and Measured the RMS Value of the Magnetic Field

This experiment is initially conducted to produce a magnetic field across the air gap, and measure it using the digital signal processing (DSP) 455 gauss meter.

The [Setup 1] is used for this experiment; the root mean square (RMS) value of magnetic flux density is taken at the DSP gauss meter. The protective circuit 1[Figure 33] is used. Only the current transformer (CT) and gauss meter are used in this setup. The coil is excited form zero amperes in the coil to higher currents up to 1.3 amperes in step of 0.1. The corresponding gauss meter values of the magnetic field density across the air gap has been tabulated. The upper arm has started to vibrate as current in the magnetic core CT's coil have reached to 1.3 amperes. The vibration of the core has stopped when the current in the coils is brought back to 0.6 amperes. From the experimental results a graph has been plotted shown in figure 14.

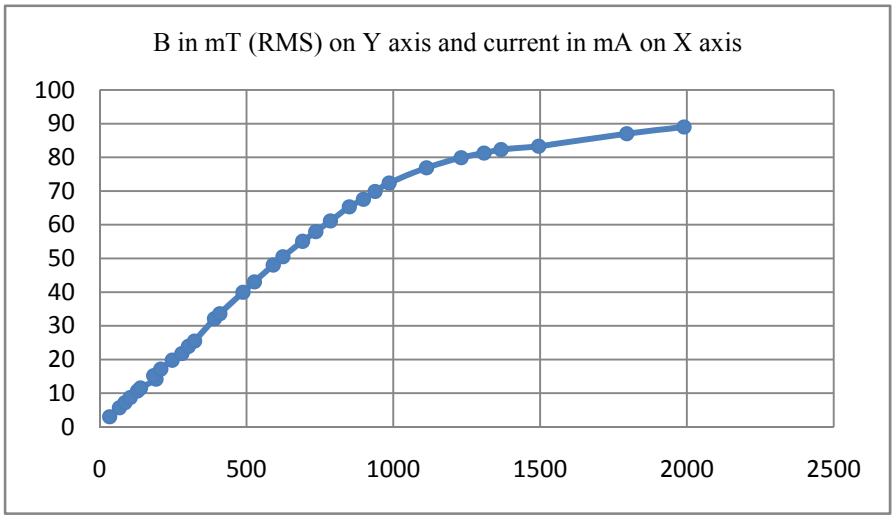

Figure 14: The graph between the RMS magnetic field and the current.

The graph has shown a linear relationship between current and the readings of the magnetic flux density at the DSP gauss meter. And we have observed a difference in the slope of the linearity above 1.1 amperes. But the saturation point of the electromagnetic core could not be determined, as the core is vibrating.

5.3 Experiment Conducted to Estimate the Magnetic Properties of the SF57 Bulk Glass

This experiment has been conduct to know how the magnetic field across the air gap would be affected by the SF57 prism. The [Setup 1] is used with the protective circuit1 [Figure 33]. The CT with the sensor and the gauss meter are used in the setup.

Initially the current (I in amperes) is applied to the coil and the RMS value of the magnetic field (B in mT) is taken without the SF57 prism glass in the air gap. Then we have repeated the same experiment with the SF57 prism placed in the air gap.

The experimental results are tabulated. The B (in mT) is the RMS value of the magnetic flux density measured by the gauss meter. The current applied (in amperes) to the excitation cables is observed on an ammeter. The graph (figure 15) is plotted with the experimental results.

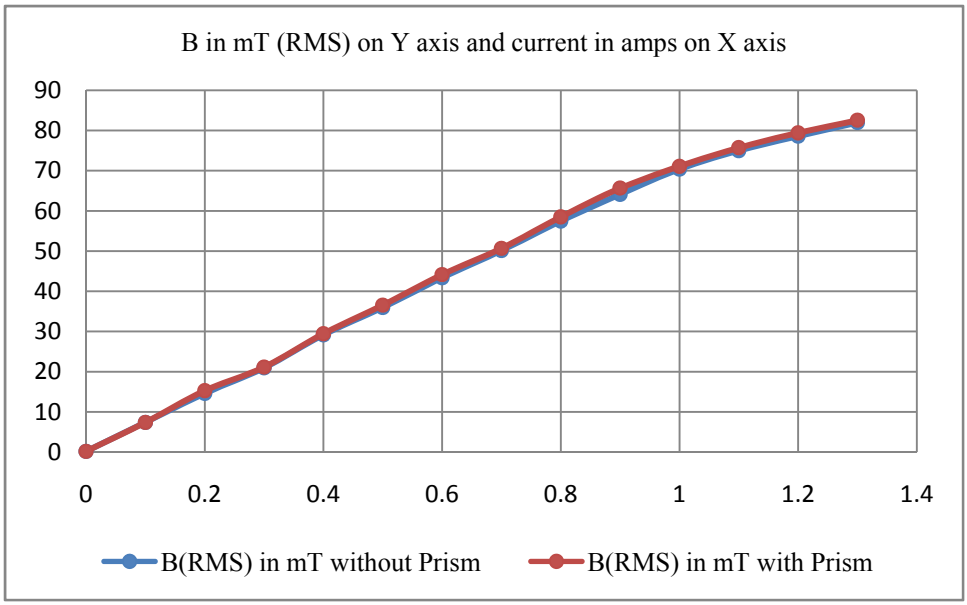

Figure 15: Graph between the current and the magnetic filed with and without pirsm.

From figure 15, there is no considerable difference in the magnitude of the magnetic flux density across the air gap, if the SF57 prism is placed in the air gap or not.

5.4 Using a Circular Magnetic Core, to Generate the Magnetic Field

This experiment has been conducted to observe the magnetic field produced by the circular magnetic core. In order to have a large dynamic range, we need to have a large linearity region. The magnetic field of the magnetic core should not get saturated. With the square shaped magnetic core we could not estimate the linearity of the setup and the saturation point is also not determined. The vibration in the square shaped core, has limited us from finding the total range. So a more stable electro magnet is constructed from a iron core, with the wire wire wound around it. A Toroid core T02091XX1 for

electro core Inc [27] is used. The [Setup 2] has been used for this experiment with no laser and chopper. The protective circuit 1 [Figure 33] has been used.

The B (in mT) is the RMS value of the magnetic field, taken across the gauss meter. The current applied (in amperes) to the excitation cables is observed on an ammeter. The experimental results obtained are plotted on a graph shown in figure 16.

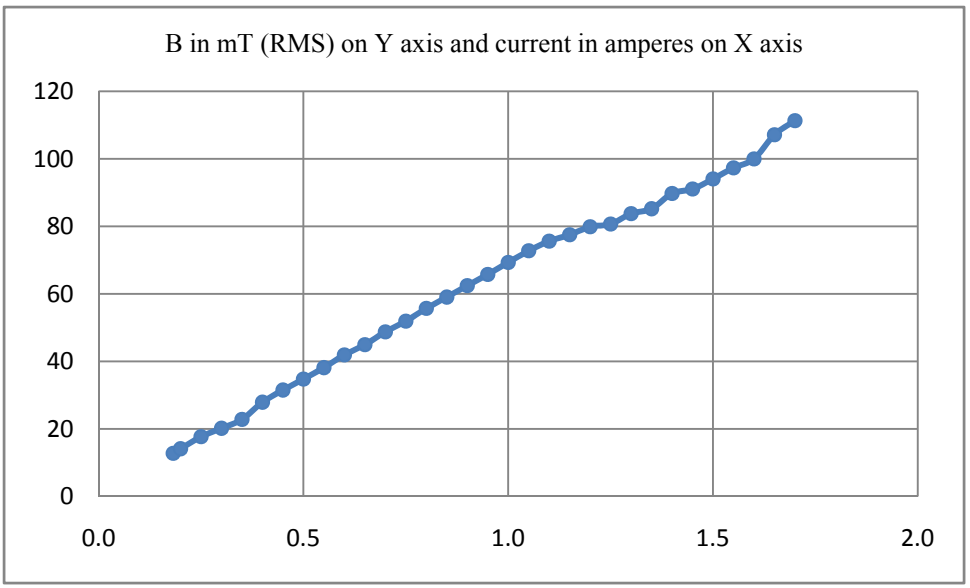

Figure 16: Graph between the current and the magnetic filed produced in the circular magnetic field.

The circular magnetic core could produce higher magnetic field across the air gap, when compared to the square shaped magnetic field. The circular magnetic core has higher range, and still it did not get saturated

5.5 Experiment Conducted to Know the Uniformity of the Magnetic Field Across the Air Gap

This experiment is conducted to know about the uniformity of magnetic field produced in the air gap. The [Setup 2] has been used for this experiment with no laser and chopper. The protective circuit 1 [Figure 33] has been used. The B (in mT) is the RMS value of the magnetic field taken on the gauss meter. The current in the coil has been kept constant and the hall probe has been initially placed at the center of the air gap. Then the probe is moved away from the center in all the directions, the corresponding magnetic field is recorded at every position.

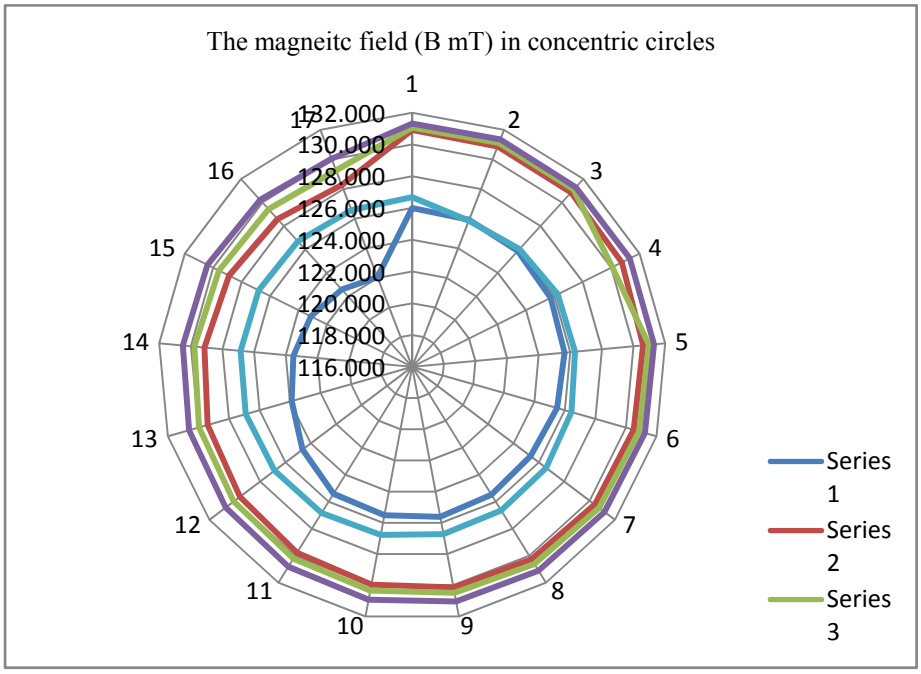

Figure 17: The graph depicting the uniformity of the magnetic field across the air gap.

Table 2: The experiment conducted to know the uniformity of the magnetic field.

				TOP 2.2 cm			
		0	0.44	0.88	1.32	1.76	2.22
	0	125.996	130.920	131.067	131.319	126.680	
	0.1764	125.931	130.882	131.120	131.356	125.863	
	0.3528	125.865	130.848	131.105	131.304	126.038	
	0.5292	125.741	130.749	130.081	131.318	126.246	
	0.7056	125.640	130.610	130.977	131.306	126.301	
	0.882	125.493	130.511	130.869	131.247	126.438	
Back 3 cm	1.0584	125.345	130.411	130.761	131.188	126.575	Front 3cm
	1.2348	125.481	130.277	130.629	131.116	126.652	
	1.4112	125.617	130.143	130.497	131.043	126.729	
	1.5876	125.512	129.966	130.358	130.929	126.784	
	1.764	125.406	129.789	130.219	130.814	126.839	
	1.9404	124.649	129.597	130.092	130.715	126.874	
	2.1168	123.892	129.404	129.964	130.616	126.908	
	2.2932	123.510	129.147	129.782	130.510	126.856	
	2.4696	123.128	128.890	129.599	130.403	126.804	
	2.646	122.590	128.588	129.434	130.226	126.691	
	2.8224	122.052	128.285	129.269	130.049	126.578	
	3		Bottom 3 cm				

From the graph and the table, we can observe that the magnetic field is strong at the outer rings, and it depletes as we move to the center. So the sensor glass prism should be kept at the center of the air gap to get exposed to maximum magnetic field.

5.6 OCS with the Line Frequency Fed to the DSP Lock in from the Gauss Meter, and Step Down Transformer

Experiment conducted to calibrate the current in the conductor using the line frequency as the reference signal from the step down transformer. We have tried various setups. Primarily we have used the chopper to chop the laser signal at a different frequency other than the line frequency, gave the chopper frequency as the reference frequency to the DSP lock in. But the output is not linear. With the increase in current there is no liner increase or decrease in the output of the difference output of the DSP lock in. We have tried to use only one photodiode, and tried the setup. But we could not still get any linear relationship between the current and the output at the DSP lock in.

So we finally thought of using the modulating frequency as the reference for the lock in. The line power is the 60 Hz voltage signal. The reference signal to the DSP lock in amplifier is taken directly from the Gauss meter. Values below 0.18 amperes cannot be taken as the DSP Lock in amplifier needs a reference signal with a voltage level of 200 mV or greater to trigger its oscillator. In order to have a 200 mV signal form the gauss meter, we need 0.18 amperes to the excitation coils of the magnetic core. Because of the 360 turns the minimum current that can be measured is 64.8 amperes.

In order to know the sensitivity and range of this current meter, we have to know the lower limit and the higher limit. A step down transformer is used to feed the reference signal of the line frequency at 60 Hz to the DSP lock in. We have used a voltage divider circuit between the transformer and the DSP reference feed, to bring down the voltage levels further to 5 V [Figure 34]. The [Setup 2] has been used for this experiment without the chopper. The protective circuit 2 [Figure 33] has been used with the 100Ω 100W resistor. The minimum current that can be attained with this setup is 0.010 * 360 = 3.6 amperes and with a step resolution of 1.8 amperes. The figure 18 is the graph obtained from the current and A-B magnitude difference values.

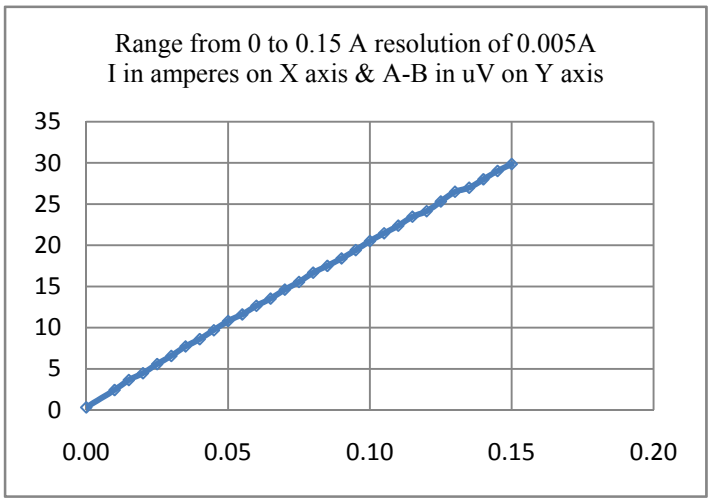

Figure 18: Graph between current and the A-B resultant value with 0.005A resolution.

To find the upper limit that the OCS can detect, the experiment same as above is repeated with the [Setup 2]. Now the protective circuit 1 is used [Figure 33] with the reference fed from the step down transformer.

Table 3: OCS readings with the line frequency from the step down transformer fed to the DSP lock in.

With both the A and B inputs connected to the DSP Lock In.

Current form 0 to 4.5 amperes

V in volts	I in amperes	A-B output in uV	B in mT
1.0	0.00	11.270	0.213
5.0	0.25	43.180	17.347
11.0	0.50	83.210	34.073
17.0	0.75	126.000	50.824
23.0	1.00	169.100	68.294
28.0	1.25	211.400	80.914
34.0	1.50	253.300	94.731
40.0	1.75	291.500	112.915
46.0	2.00	330.800	136.782
51.0	2.25	376.800	153.891
57.0	2.50	417.200	171.674
63.0	2.75	463.500	188.725
69.0	3.00	504.100	206.324
75.0	3.25	538.600	222.371
81.0	3.50	564.000	240.324
87.0	3.75	607.000	258.431

V in volts	I in amperes	A-B output in uV	B in mT
92.0	4.00	660.000	275.621
98.0	4.25	742.000	293.091
104.0	4.50	806.000	310.060
110.0	4.75	Fuse of the variac got blowed off.	

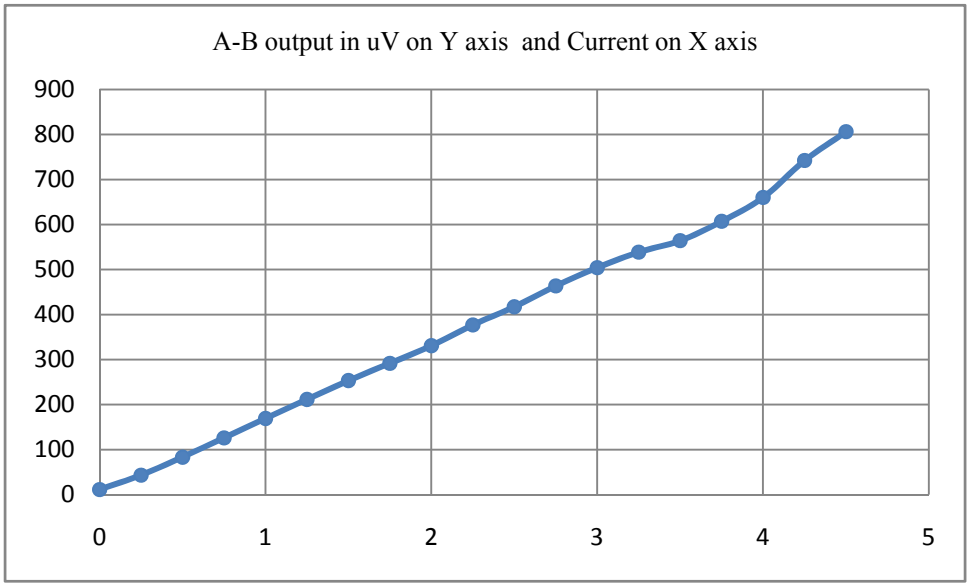

Figure 19: Graph between current and the A-B resultant value with the reference fed from the step down transformer to the lock in.

Figure 19 shows a linear relationship between the current applied and the A-B magnitude difference value. A minimum current of 1.8 amperes and the maximum current of 1620 (4.5 * 360 = 1620) amperes has been achieved with this OCS. The fuse of

the variac got burnt when the current in the coil reached about 4.5 amperes. The cores magnetic field didn't get saturated.

5.7 Experiments Conducted to Know how the Path Length of the Laser Beam in the Sensor Glass Affects the Outcome

Convincing results have been obtained, that if there is an increase in the current there is a liner increase in the difference output of the DSP lock in amplifier. Now experiment is conducted to estimate how the path lengths of the laser beam inside the sensing prism affect the output at the DSP lock in amplifier magnitude value. The [Setup 2] is used with the protective circuit 1 [Figure 34]. We didn't use the chopper. The reference frequency is fed from the step down transformer. The current in the coil is incremented, and the output of the DSP lock in is plotted on the graph. The laser path length is adjusted to be large, average and small. And the differential output is also correspondingly large, average and small.

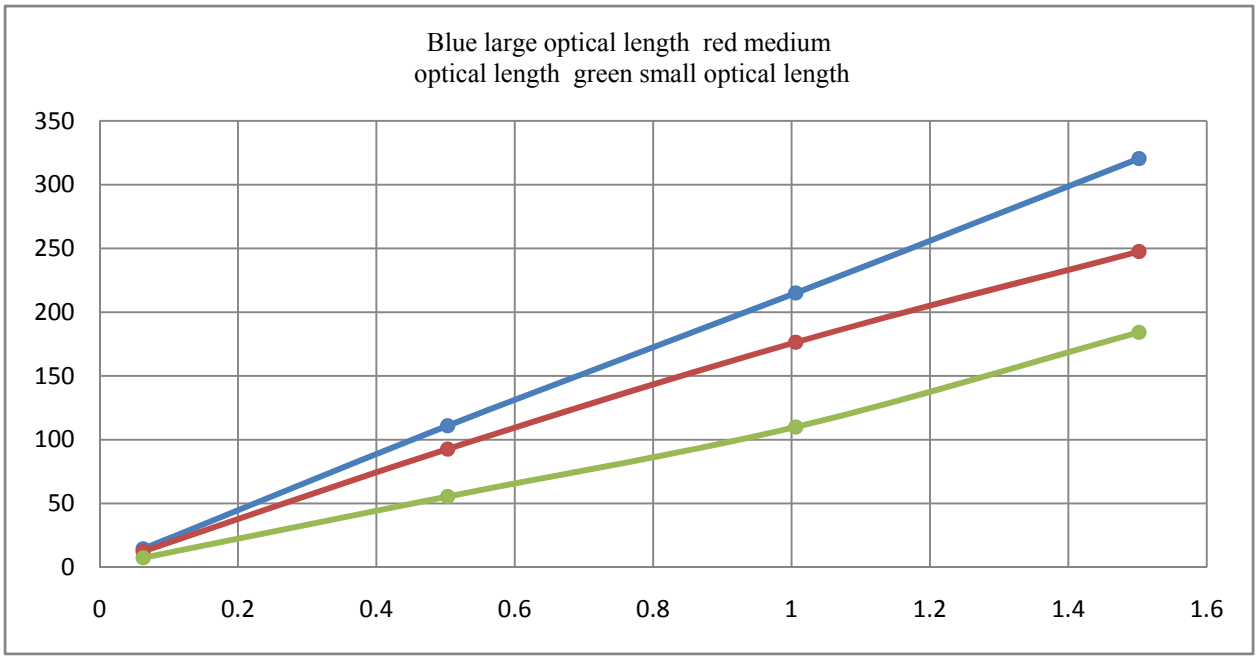

Figure 20: Graph between current and A-B resultant value, with different path lengths.

From the figure 20, one can conclude that the more the path length in the sensor glasses travels the more the rotation of the plane of polarization the light experiences.

5.8 Use of Multiple Path Length Using Multiple Prisms

The magnitude of the rotation depends upon the strength of the magnetic field, the nature of the transmitting substance, and Verdet constant, which is a property of the transmitting substance, its temperature, and the frequency of the light. The direction of rotation is the same as the direction of current flow in the wire of the electromagnet, and therefore if the same beam of light is reflected back and forth through the medium, its rotation is increased each time.[17]

With this knowledge we tried of using a multiple path prism, which will in turn increase the optical path length. We have employed 3 prism in with one is placed above the other, and the third one is placed diagonally to connect the top and bottom prisms. The [Setup 2] with the protective circuit 1 [Figure 33] has been used. The single prism is replaced with a double path length made of 3 prisms. The reference signal has been applied from the step down transformer. The experimental results thus obtained are plotted on to the graph (figure 21).

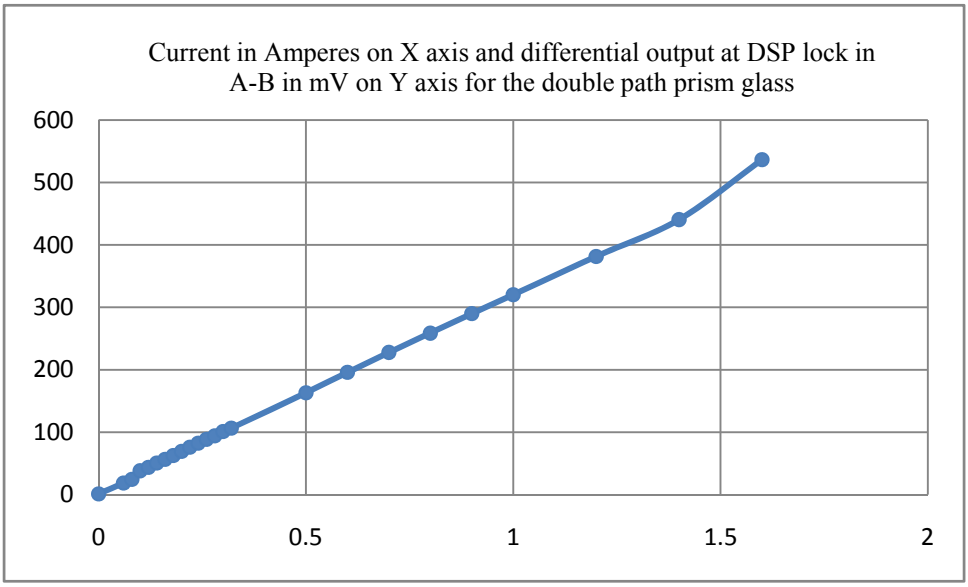

Figure 21: Graph between current and A-B resultant value, with double path length 3 prisms setup.

The results indicated that the output of the 3 prism double path length setup increase by one and half, when compared to the singe prism path.

5.9 Experiment Conducted to Simulate the Actual Setup Using a Double Loop Welding Cable, and a Single Current Transfomer to Generate the Current

Until now we have used the 360 turns of wire around the circular magnetic core. But now we would like to see how an actual current carrying conductor can generate magnetic fields in a magnetic iron core. The [Setup 4] is used with one CT acting as the current generator. The welding cable has been used as the current carrying conductor. The laser and the DSP lock in are not used. The current applied to the CTs is recorded, and the current generated in the conductor loop is measured with the help of a CT ammeter. The magnetic flux density B is calculated in B mT. The experimental results are plotted on the graphs (figures 22 and 23) with the magnetic field on y axis and the current at in the loop, and current fed to the CTs on X axis respectively.

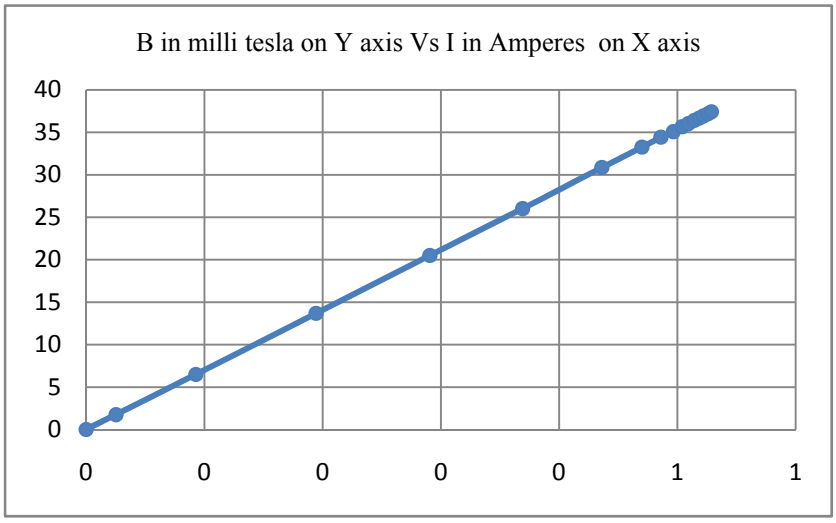

Figure 22: Graph between current measured in the wire and the magnetic field produced.

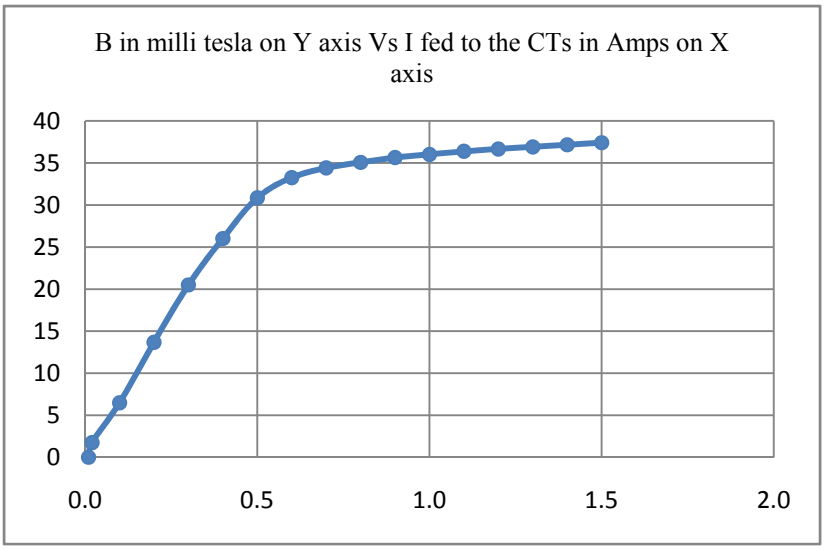

Figure 23: Graph between current fed into the CT to generate current and the magnetic field produced.

The graph (figure 23) shows that the magnetic field generated by the CT got saturated and they could not generate any more current in the coil. But the magnetic core is not yet saturated. In the other graph (figure 22), there is a linear relationship between the magnetic field and the current generated in the loop. So the magnetic core is not saturated.

Now instead of double loop through the CTs used for generations of magnetic field; a single loop is used. The double loop setup generated more magnetic field in the air gap when compared to the single loop setup.

5.10 Experiment Conducted to Simulate the Actual Setup Using a Double Loop Welding Cable, and a Three Current Transformers to Generate the Current

We thought of increasing the number of CTs to generate more current into the coil. The [Setup 4] is used with 3 CTs used for generating the current. The welding cable has been used as the current carrying conductor. The graph (figure 24) between the current in the loop and the magnetic field produced.

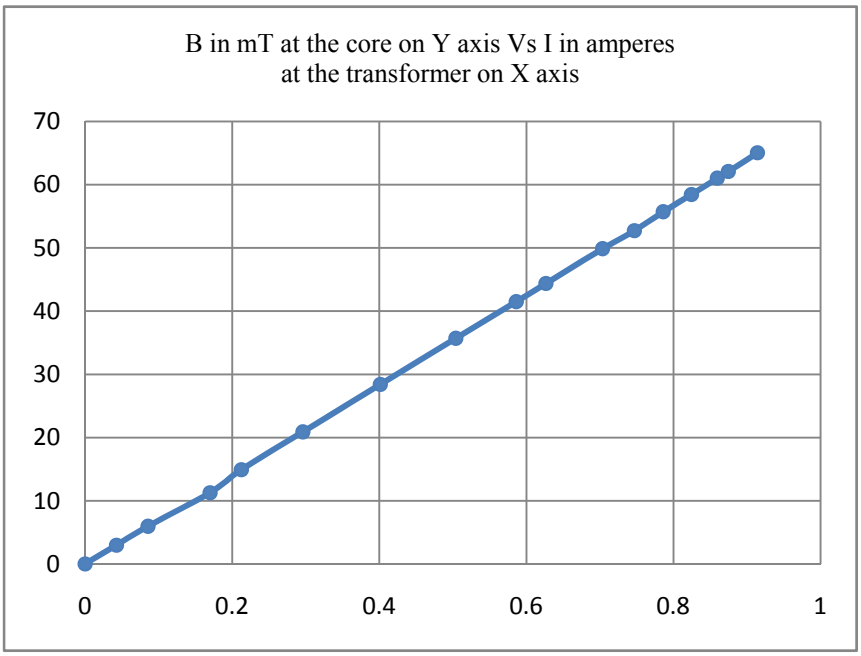

Figure 24: Graph between current measured in the wire using 3 CTs as generators and the magnetic field produced.

Even here the 3 CTs that are used for current generation got saturated. The magnetic core's magnetic field did not get saturated. The current in the 3 CTs configuration has increased when compared to the 1 CT configuration.

5.11 Experiment Conducted to Simulate the Actual Setup Using a Single ¾ Inch Cable, and a Three CTs to Generate the Current

So we thought of using a much thicker wire than the present cable to increase the current in the conductor. We used a ¾ inch cable as the current carrying conductor in the [Setup 4] with 3 CTs used as the generators. The actual experimental setup is show in the figure 25 below.

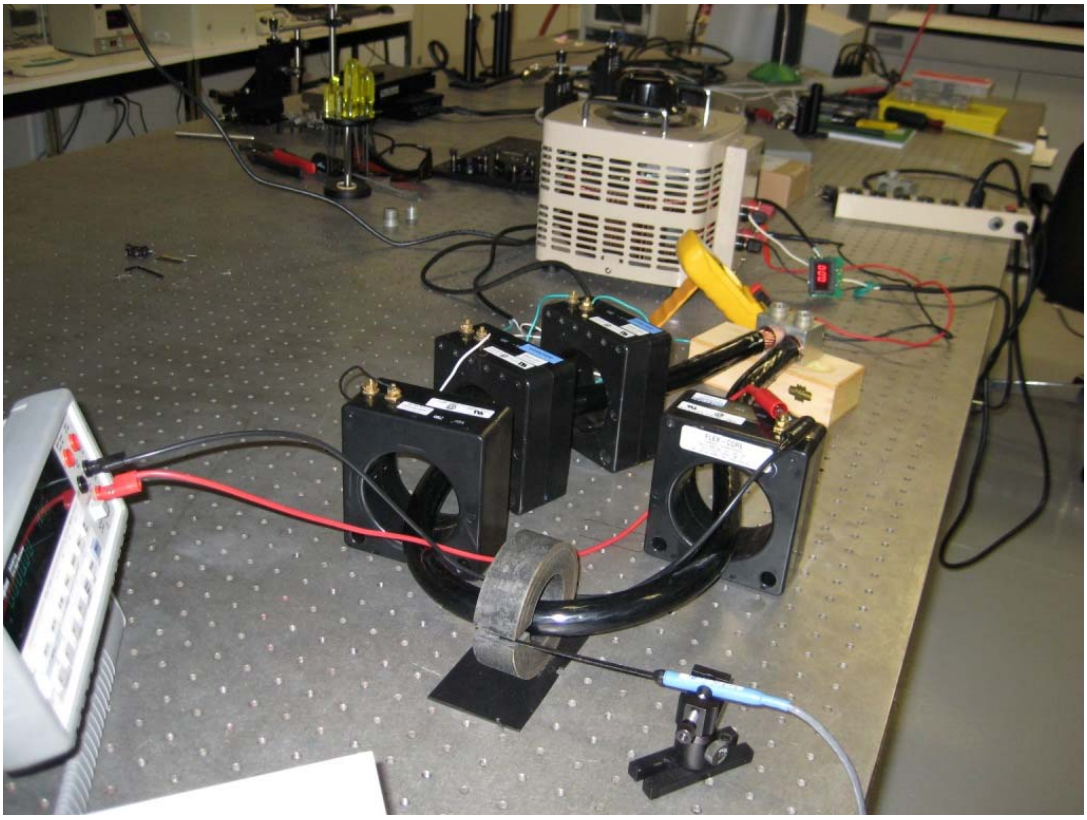

Figure 25: The actual setup in the optics lab with the ¾ inch cable and 3 CTs to generate the current and one to measure the current.

When compared the welding cable the magnetic field generated across the air gap is more, when the ¾ inch cable is used. The experimental results are plotted on the graph (figure 26) with the current in the loop taken on x axis and magnetic field on y axis.

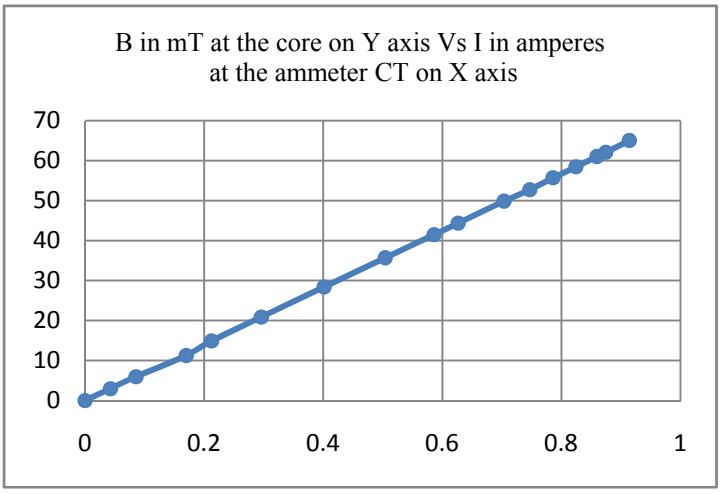

Figure 26: Graph between current produced in 3/4 inch wire and the magnetic field, with 3 CTs used to generate the current.

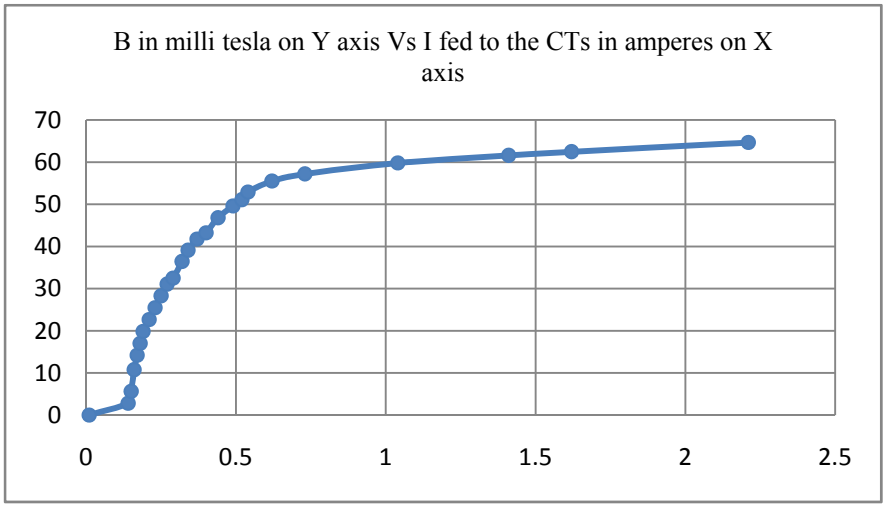

Figure 27: Graph between current fed in to the 3 CTs in the .3/4 inch wire and the magnetic field

Still the magnetic core is not yet saturated. But the current generating CTs got saturated. The graph (figure 27) between the current given to the CTs Vs the magnetic field produced depicts this. The ¾ inch cable can generate more current than the welding cable.

5.12 Experiment Conducted to Observe how the Resultant A-B Readings at the DSP Lock in Varies with the Change in Temperate and Current, while Feeding the Line Frequency as the Reference

The experiment is conducted to observe how the resultant magnitude at the DSP lock in amplifier is varied when both the current and temperature are varied. The [Setup 3] with the protective circuit 1 [Figure 33] is used. The reference value is applied from the step down transformer.

Initially the temperature is fixed, and current is applied to the magnetic core's coils from the variac. For a range of currents the corresponding DSP lock in amplifier difference readings are recorded. Then the temperature is incremented in steps, and has repeated the experiment for every temperature step; of taking the difference reading at the DSP lock in for the range of currents. Then the results are tabulated. This gives the values for the database. The graph (figure 28) is plotted from the experimental results with the

temperate on Y axis and the resultant difference value on X axis. The value in the square brackets is [Temperature in degrees Celsius]

Table 4: Reading taken at the A-B resultant value, with the current and the temperature changing.

	temperature	23	27	35	40
		A-B uV	A-B uV	A-B uV	A-B uV
V	I in amperes	[23]	[27]	[35]	[40]
3	0.062	4.8	4.8	4.8	4.8
5	0.1	7.4	7.4	7.4	7.4
12	0.2	16	16	16	16
18	0.3	24.3	24	24	24
24	0.4	32.7	32	31.7	31.2
31	0.5	40.7	40.1	39.6	39
37	0.6	48.6	48	47.5	47
44	0.7	56.7	56	56.5	55
50	0.8	65.8	65.1	63.3	62.1
57	0.9	73.9	73	72	70
64	1	81.8	81.5	81	80
70	1.1	89.9	89	88.5	88
82	1.2	98.5	98	97	95
89	1.3	106.3	106	105.1	103

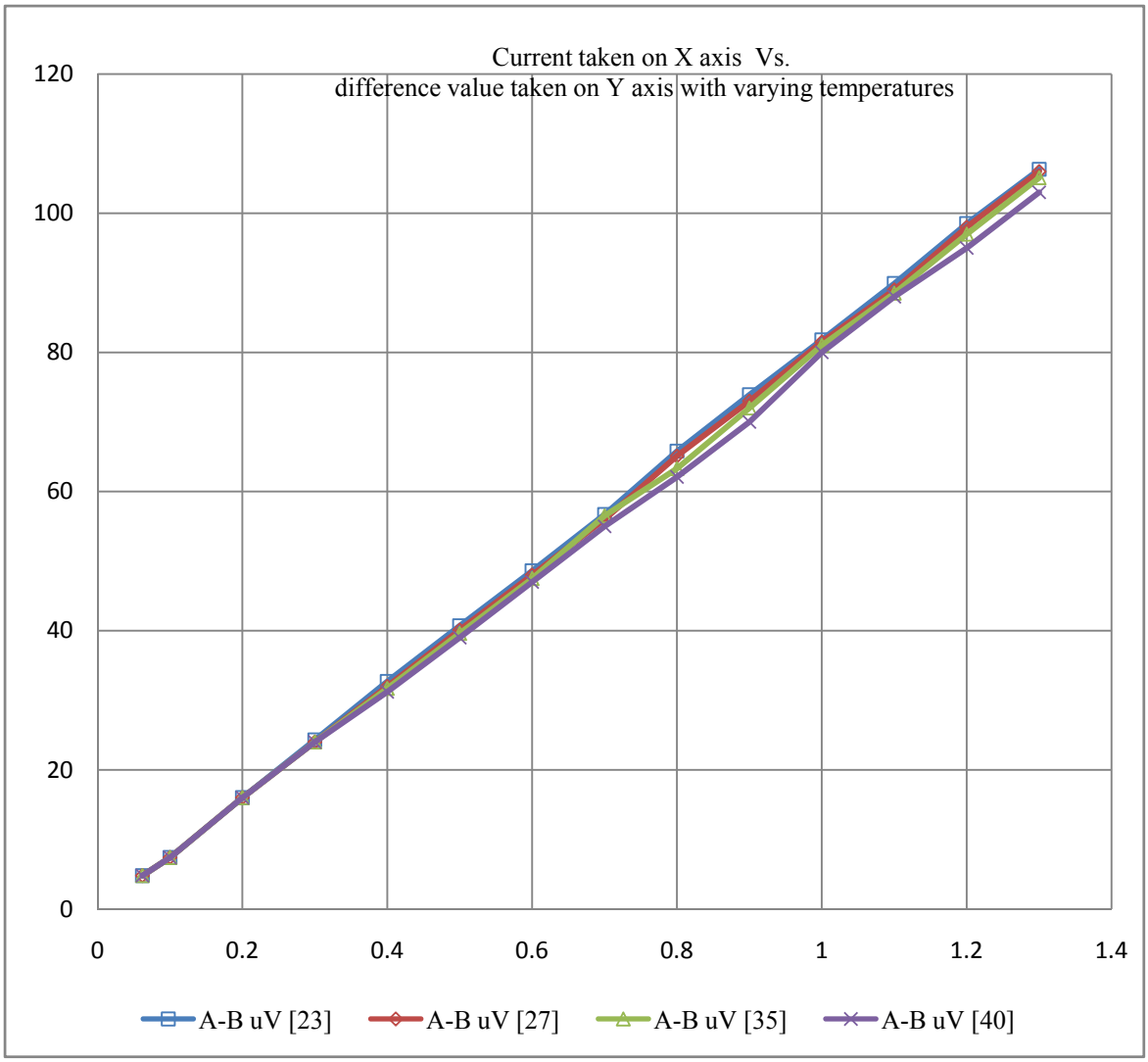

Figure 28: Graph between the current and the A-B resultant values, at various temperatures.

The graph (figure 28) and the results show that the resultant magnitude value at the DSP lock in changes, when there is a variation in the temperate. To compensate for this change, we have to determine the temperature using the dual frequency method. And then the lookup table method is used to compensate the changes.

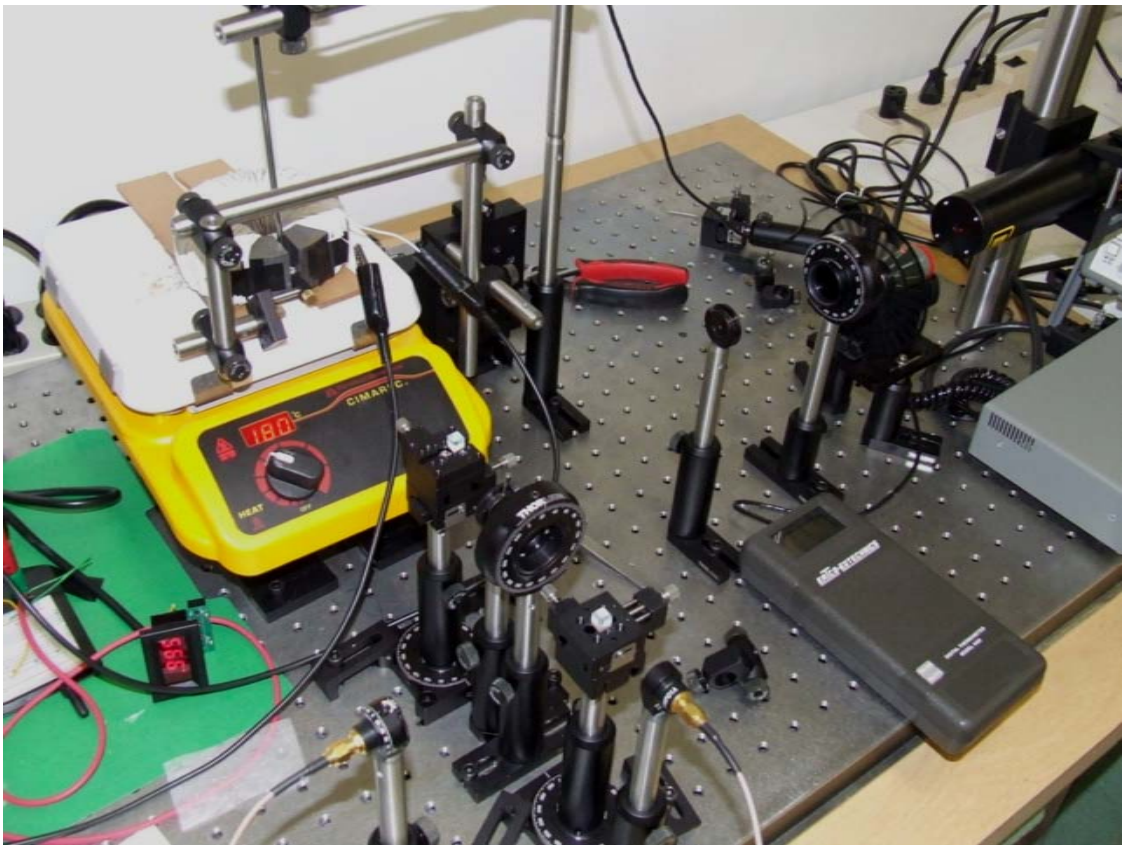

Figure 29: The OCS setup mounted on a hot pan to change the temperature.

The actual experimental setup (figure 29) used for the heating of the core and prism. The core and prism place on the hot plate. The laser, PBS's, half wave plate and the photo diodes layout can be seen in the picture.

5.13 Experiment Conducted to Observe Readings of the DSP Lock in when there is a Change in Temperate at a Constant Current, while Feeding the Function Generator Sync as the Reference

This experiment is conducted to sense the temperature around the sensor. The [Setup 3] is used with the protective circuit 1 [Figure 33]. The reference signal is applied form the function generator. The coil around the magnetic core is excited by the function generator, instead of the variac. Frequency and voltage of the function generator are fixed to Sine wave 367 Hz, 10 V_{p-p} respectively. And a constant current of 0.03078 amperes is applied.

The temperatures around the sensor are changed with the aid of the hot plate. And A-B resultant magnitude difference values are recorded at regular intervals on DSP lock in amplifier. As the current is constant, and the changes in the difference value only reflect the temperature changes. The temperature is taken in degrees Celsius.

Table 5: Experiment conducted with the current kept constant and the temperature varying with the reference from the function generator.

Temperature ^{o}C	A-B uV
22.6	6.352
23.53	6.324
24.5	6.295
26.75	6.265
28.79	6.183

30 6.118

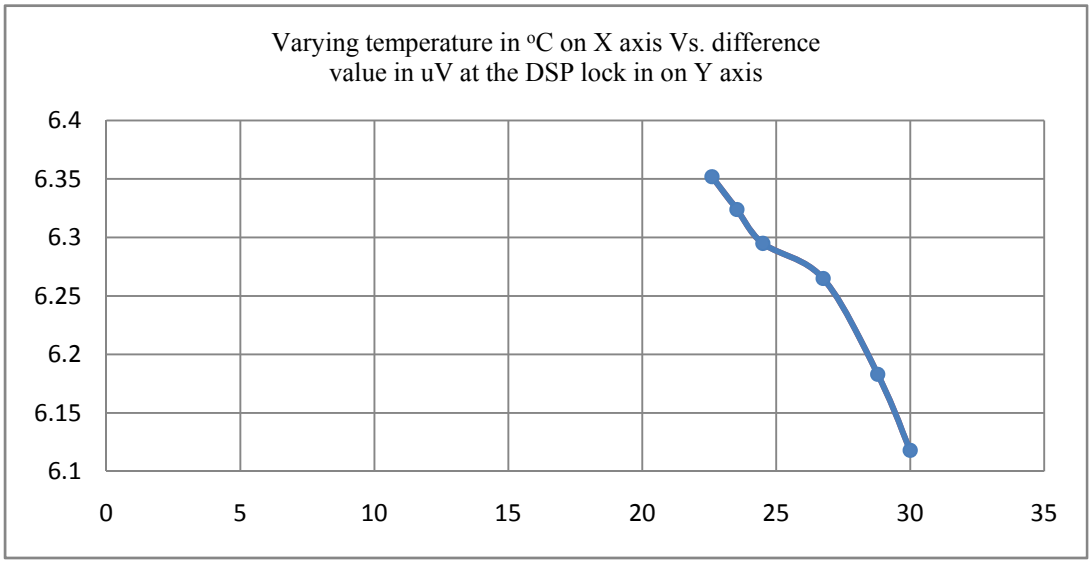

Figure 30: Graph between temperature around the OCS and the A-B resultant value at the DSP lock in with the reference from the function generator.

The graph in figure 30 is plotted from the experimental results. From the graph, as the temperature increases the magnitude difference value at the DSP lock is decreases, though the current is kept constant. These values are initially fed into the data base.

When the OCS is used in the sensing mode, the readings from the temperature sensor are used to lookup at the index of the database values. Then the readings form current senor are compared to the database, which gives the accurate current readings.

5.14 Experiment Conducted to Observe how the Readings at the DSP Lock in Varies with the Change in Temperate a Particular Current, while Feeding the Line as the Reference

The same experiment as above is conducted, by keeping the current constant and varying the temperature with the help of the heating pan. But this time the line voltage is applied as the reference signal to the DSP lock in amplifier form the Step down transformer. The excitation to the coil is fed from the variac. This will give us a close observation of how the current reading will change with in temperature. Temperature is taken in degrees celsius. The current in the coil is kept constant at 1 ampere.

Table 6: Experiment conducted with the current kept constant and the temperature varying with the reference from the line frequency.

Temperature	A-B uV
24.6	131.68
25	130.46
26	129.07
27.3	127.96
29	126.42
31	125.86
33.49	124.18

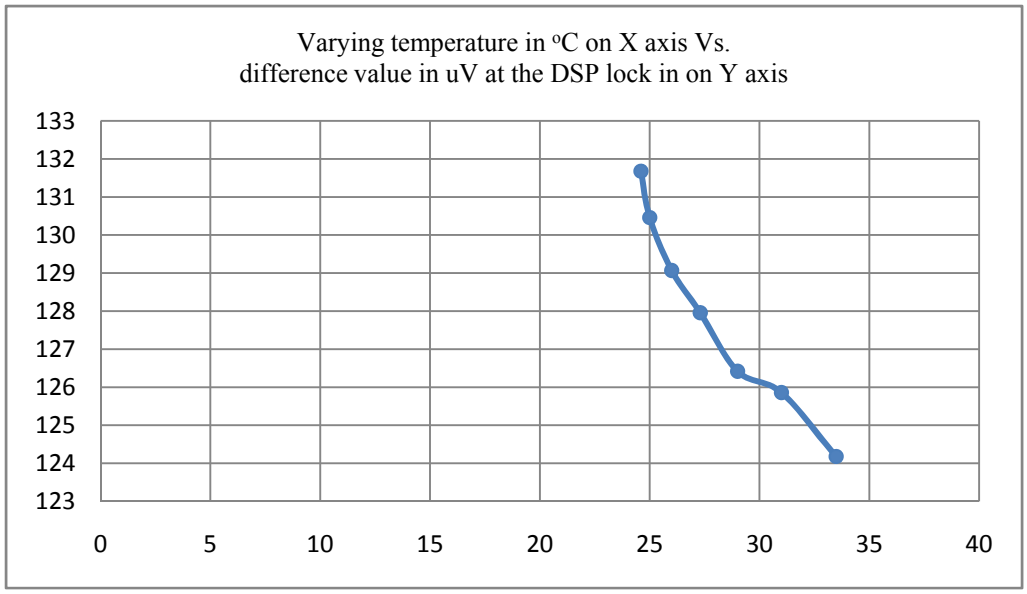

Figure 31: Graph between temperature around the OCS and the A-B resultant value at the DSP lock in with the reference from the line frequency.

As the temperature increase around the sensor the difference value at the DSP lock is decreasing. This gives us a closer look of how the current reading varies, when there is a change in the temperature. And this emphasizes the importance to compensate for temperature changes.

5.15 Experiment Conducted to Observe how the Readings at the DSP Lock in Varies with the Change in the Frequency of the Excitation Coil while keeping the Temperature and Current in the Coil Constant

Finally, another experiment is conducted to understand the effect of the change in the excitation frequency of the coil around the magnetic core. For estimating the effect of frequency change, the current and the temperature are kept constant and the resultant magnitude at the DSP lock in amplifier is observed.

The [Setup 3] is used with the protective circuit 1 [Figure 33]. The reference signal is taken from the function generator, and the coils of the circular core are also excited by the function generator. The temperature is kept constant and the current is kept constant at 0.03078 amperes (the maximum the function generator can produce). The frequency of the function generator is changed, and this change the frequency of the magnetic field produced. This has an effect on the output though the current and temperature are constant. The resultant magnitudes at the DSP lock in amplifier are tabulated at the respective frequencies. And from these values the graph is drawn.

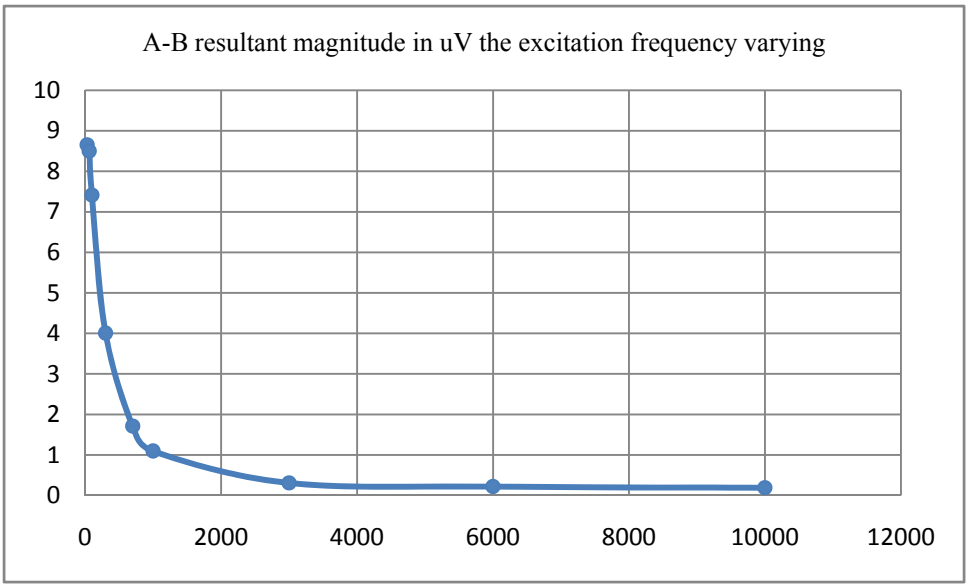

Figure 32: The graph between the excitation frequencies and the resultant magnitude at the DSP lock in.

The graph (figure 32) above is plotted from the experimental results. The figure 32 depicts an exponential decrease in the resultant magnitude output of the DSP lock in, with increase in frequency. So it is better to operate at lower frequencies, to yield a large resultant difference value.

CHAPTER 6

CONCLUSIONS

An optical current sensor OCS that is capable of measuring both the current and the temperature has been successfully designed. Two distinct dual frequency sources have been used, for measuring the two parameters. The resultant magnitude difference value at the DSP lock in amplifier reflects the change in the current or temperature, or both. It depends on the reference value fed to the lock in amplifier. A matrix of values is obtained when the OCS is in controlled conditions. Then these values are entered into the database. And when the OCS is in the sensing mode, the temperature and current resultant magnitude values at the digital signal processing DSP lock in amplifier are used to look up, at the index and the actual current readings from the database. So the temperature compensation of the OCS is achieved.

The major Outcomes of the experiment are

1. The maximum measured current, which is limited by the vibration of the magnetic core (360 turns) setup, is 1620 ampere root mean square (RMS). The smallest current that can be measured is 0.36 A, which is limited by the resolution of the ammeter.

2. The actual setup is simulated using a ¾ inch wire loop, and current transformers (CT)s are used to generate the current in the loop. With this setup maximum of 363 amperes is generated with the ¾ inch loop setup.
3. Measured magnetic flux densities have show agreement with the simulation results. Multiple reflections of the laser path in the SF57 sensor glass has increase the resultant difference value of the two photo diodes at the DSP lock in.
4. The current in the current carrying coil is detected as the resultant magnitude difference value on the DSP lock in amplifier. The temperature around the sensor is also measure, using a different source to generate the magnetic field. And have proposed new methods to compensate the temperature changes on the current readings.
5. At constant current, with the increase in the temperature the resultant difference value of the two photo diodes at the DSP lock in amplifier is decreasing.
6. At constant temperature and current, with an increase in the excitation coil power supply frequencies, the resultant difference value of the two photo diodes on the DSP lock in amplifier is decreasing.

Future work

The OCS developed in our lab has not been tested for the entire ranges. The maximum current that the OCS can measure is still not determined as we could not produce enough current in the coil. The OCS has not been tested for a larger temperature ranges. Negative temperature response of the OCS has not been

determined. In the present setup, the effect of temperature on the magnetic core and the SF 57 prism glass are only determined. Negative temperatures are not applied due to the unavailability of a temperature controlled arena. The combined effect of temperature on the other components like the PBS, half wave plate, photo diodes and the laser are to be determined. Other simple methods to compensate the temperature effect by using the temperature and current database can be proposed.

APPENDIX

MATLAB CODE AND SET-UPS

Figures

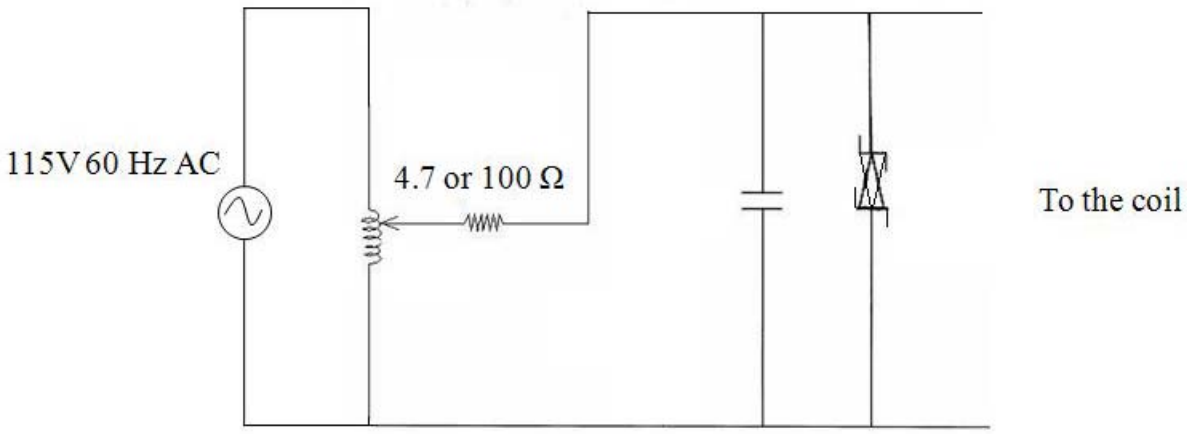

Figure A.1: Protective circuit connected between the power source variac and the excitation coils of the magnetic core.

Protective circuit 1

Uses the 4.7Ω 6.2W resistor in series, with a capacitor, transient suppressor and the load connect in parallel. With this circuit in the setup, more current can be forced into the coil, while controlling the resolution or the incrementing the current in steps becomes hard to control. This circuit helps us to find the maximum dynamic range of the OCS.

Protective circuit 2

Uses the 100Ω 10W resistor in series, with a capacitor, transient suppressor and the load connected in parallel. With this circuit in the setup, the maximum current that can be supplied into the circuit is limited, but the best resolution of the OCS can be determined, as the current in the coil can be made to increment or decrement in small steps.

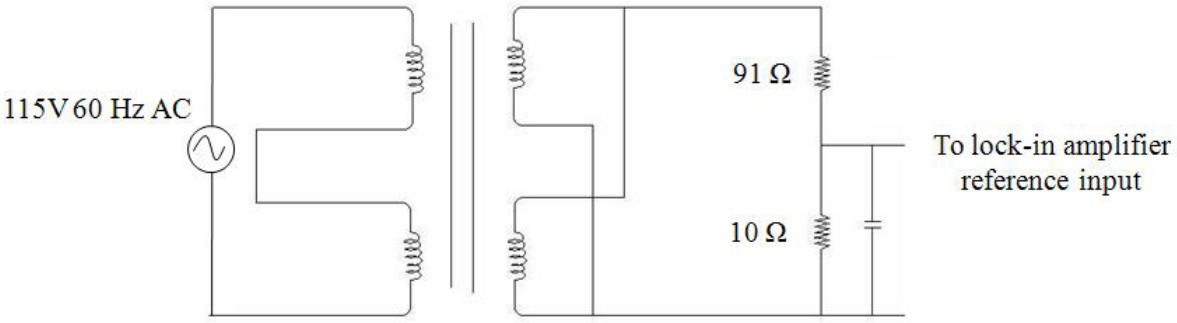

Figure A.2: Circuit placed between the step down transformer and the line frequency reference signal of the DSP lock in amplifier.

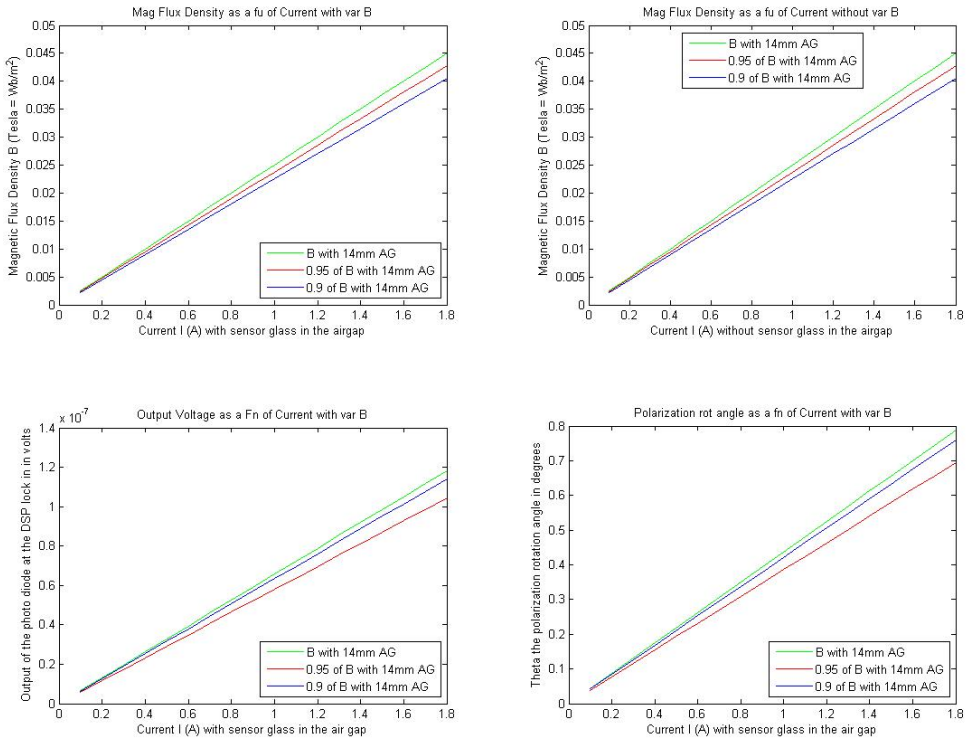

Figure A.3: Matlab simulated graphs.

Matlab Code

```
clear all;% All units in SI system

Lmcr=35.9918*10^-3;

%    Length of the magnetic core radius in meters (35.9918 in mm)*10^-3

%    Core No. 3698 G 3304 0750  from Electro-Core

Lcore=2*pi*Lmcr;
```

```
%   Length of the magnetic core perimeter in meters  22.7*10^-3
Uo=4*pi*10^-7;
% permeability of the vaccume is 4*pi*10^-7 N*A^-2
Uhsr=1;
%    Permeability of the Hall Sensor 0.260/0.248 of the SF57 bulk glass    H/m  =
Kg*m*s^-2*A^-2 = N*A^-2
Uhs=Uhsr*Uo;
%    Relative Permeability of the Hall Sensor  U = Uo*Ur
Umcr=125;
%    Permeability of the Magnetic Core 125     H/m  = Kg*m*s^-2*A^-2 = N*A^-2
Umc=Umcr*Uo;
%    Relative Permeability of the Magnetic Core
Uhsair=4*pi*10^-7;
%   Permeability of the air without the hall sensor in the air gap;
Uhsairr=Uhsair./Uo;
%    Relative Permeability of the air without the hall sensor in the air gap;
VCrad=21.8;
VCdeg = (VCrad*180)/pi;%UNITS degrees*T^-1*m^-1
Lairgap=14*10^-3;
%   Length of the air gap in meters 6.5*10^-3
Lairgap1=13*10^-3;
Lairgap2=15*10^-3;
```

```
Lmcct=29.9974*10^-3;
%   Length of the magnetic  core thickness in meters 28.575*10^-3
Lmccw=21.9964*10^-3;
%   Length of the magnetic core width in meters 15.875*10^-3
Aairgap=(Lmcct+Lairgap).*(Lmccw+Lairgap);
%   Cross Sectional Area of the air gap in meters2
Aairgap1=(Lmcct+Lairgap1).*(Lmccw+Lairgap1);
Aairgap2=(Lmcct+Lairgap2).*(Lmccw+Lairgap2);
Amccs=Lmcct*Lmccw;
% Cross Sectional Area of the Magnetic Core in meters2
n=360;
%   number of turns of the coil
I=0.1:.1:1.8;
%    current in the coil(range 5 to 1700) in amperes
B=((Uhs*n*I)./((Lcore*Uhs*Aairgap./Umc/Amccs)+Lairgap-
(Lairgap*Uhs*Aairgap./Umc/Amccs)));
% Magnetic Flux Density Units( tesla = Wb/m^2 = Kg*s^-2*A^-1 = N*A^-1*m^-1) ....
in CGS system gauss
%B1=((Uhs*n*I)./((Lcore*Uhsr*Aairgap1./Umcr/Amccs)+Lairgap1-
(Lairgap1*Uhs*Aairgap1./Umc/Amccs)));
%B2=((Uhs*n*I)./((Lcore*Uhsr*Aairgap2./Umcr/Amccs)+Lairgap2-
(Lairgap2*Uhs*Aairgap2./Umc/Amccs)));
```

```
%calculation of new B
Rmccore = Lcore./(Uo*Umcr*Amccs);
%reluctance of the magnetic core
Rairgap = Lairgap./(Uo*Uhsr*Aairgap);
%reluctance of the airgap
NB = ((n*I)./(Aairgap*(Rmccore + Rairgap)));
%calculation of Magnetic Flux Density directly
Bair=((Uhsair*n*I)./((Lcore*Uhsairr*Aairgap./Umcr/Amccs)+Lairgap-
(Lairgap*Uhs*Aairgap./Umc/Amccs)));
% Magnetic Flux Density in the airgap "without" the sensor glass    Units( tesla =
Wb/m^2 = Kg*s^-2*A^-1 = N*A^-1*m^-1) .... in CGS system gauss
H=((n*I)./((Lcore*Uhsr*Aairgap./Umcr/Amccs)+Lairgap));
%Magnetic field intensity  Units    ( A*m^-1 ) ... in CGS sysstem oersteds
%H1=((n*I)./((Lcore*Uhsr*Aairgap1./Umcr/Amccs)+Lairgap1));
%H2=((n*I)./((Lcore*Uhsr*Aairgap2./Umcr/Amccs)+Lairgap2));
B1=0.95*B;
B2=0.9*B;
theta=VCrad.*B.*Lairgap;
%calculation of the Theta the polarization rotation angle  Units radians(SI)
theta1=VCrad.*B1.*Lairgap1;
theta2=VCrad.*B2.*Lairgap2;
thetadeg=VCdeg.*B.*Lairgap;
```

```
%calculation of the Theta the polarization rotation angle  Units degrees
thetadeg1=VCdeg.*B1.*Lairgap1;
thetadeg2=VCdeg.*B2.*Lairgap2;

%output power
Laservoltage = 8.6*10^-6;
output = Laservoltage.*sind(thetadeg);
output1 = Laservoltage.*sind(thetadeg1);
output2 = Laservoltage.*sind(thetadeg2);
x=I;
y=B;
subplot(2,2,1),plot(x,y,'g',x,B1,'r',x,B2,'b')
%  plot between magnetic flux density B on Y axis and with the variable current on X
axis
xlabel('Current I (A) with sensor glass in the airgap');%labling the x axis
ylabel('Magnetic Flux Density B (tesla = Wb/m^2)')%labling the y axis the units should
be amperes per meter
title('\fontname{arial}Mag Flux Density as a fu of Current with var B','fontsize',10);
legend('B with 14mm AG','0.95 of B with 14mm AG','0.9 of B with 14mm AG',0);
subplot(2,2,2),plot(x,B,'g',x,B1,'r',x,B2,'b')
%  plot between magnetic flux density B on Y axis and with the variable current on X
axis
```

```
xlabel('Current I (A) without sensor glass in the airgap');%labling the x axis
ylabel('Magnetic Flux Density B (tesla = Wb/m^2)')%labling the y axis the units should be amperes per meter
title('\fontname{arial}Mag Flux Density as a fu of Current without var B','fontsize',10);
legend('B with 14mm AG','0.95 of B with 14mm AG','0.9 of B with 14mm AG',0);
subplot(2,2,3),plot(x,output,'g',x,output1,'r',x,output2,'b');
%   plot between Theta the polarization rotation angle (Radians) as a function of Current
X label('Current I (A) with sensor glass in the air gap');%labling the x axis
Y label('Output of the photo diode at the DSP lock in in volts')%labling the y axis the units should be radians
title('\fontname{arial}Output Voltage as a Fn of Current with var B','fontsize',10);
legend('B with 14mm AG','0.95 of B with 14mm AG','0.9 of B with 14mm AG',0);
subplot(2,2,4),plot(x,thetadeg,'g',x,thetadeg1,'r',x,thetadeg2,'b');
%   plot between Theta the polarization rotation angle (Degrees) as a function of Current
xlabel('Current I (A) with sensor glass in the air gap');%labling the x axis
ylabel('Theta the polarization rotation angle in degrees')%labling the y axis the units should be degrees
title('\fontname{arial} Polarization rot angle as a fn of Current with var B','fontsize',10);
legend('B with 14mm AG','0.95 of B with 14mm AG','0.9 of B with 14mm AG',0);
```

Setup 1

The square shaped magnetic core current transformer (CT) from Flex-Core (multi ratio transformer Model 331-200) [28] is used. The CT is supplied with a removable leg. The leg is separated from the CT, and a gap of 14 mm in length is cut at the center, and the leg is placed back. This creates the room for the sensor glass SF 57 prism to be placed in air gap of the square CT where the magnetic field is produced. The magnetic field in the CT is produced by passing current through the CT coil. The CTs red/white and green/white wires are connected to a variac, with whom the flow of current in the CT's coil is controlled. A protective circuit [Figure 33] is placed between the variac and CT's coil, to short circuit any electrical surges or peaks. Either a 4.7Ω 6.2W or the 100Ω 100W resistor is placed in series, with a capacitor, transient suppressor and the load in parallel. Changing the resistor helps us in getting a better dynamic range or better resolution. An ammeter is also place in series, to calculate the current flowing through the coil. A volt meter is place across the variac to calculate the voltage. The units of current and voltage are in amperes and volts respectively.

The Hall probe of the Lakeshore digital signal processing DSP 455 gauss meter is placed in the air gap of the CT. The magnetic field produced in the air gap of the CT is displayed on the gauss meter. The gauss meter is kept in auto range mode. The root mean square RMS value of the magnetic field is taken at the gauss meter. The magnetic field B is calibrated in milli tesla (mT). The laser light is being focused on to the first polarization beam splitter PBS (polarizer) through a 20A filter. From the first PBS, the

light is incident on the SF57 prism sensor glass in the air gap of the CT. The laser light is modulated by the magnetic field, and is then reflected back from the sensor prism on to the half wave plate. The half wave plate is rotated at an angle of 22.5 degrees. The laser light passes through the half wave plate and falls on the second PBS (analyzer). The laser light is split into vertical and horizontal components.

The light intensity of each component is converted into electrical signal by the two SM05PD1A photo diodes. The electrical signal from the two photo diodes are connected to the inputs of SR 830 DSP lock in amplifier. The DSP lock in amplifier displays the resultant magnitude in volts. The difference between the two photo diodes are calculated, when the DSP lock in is in A-B mode at the signal input. The settings at the lock in are set as follows. No line is applied at the filter setup. The time constant is set to 1s with 12 dB slope/oct. The sensitivity setup is adjusted by the auto gain function. The reserve is set to low noise. The channel one display is set to R (resultant) with no off set. The interface and others are set to default setting. The source at the reference is kept at the internal. The reference signal to the lock in is applied at the REF IN. The reference signal may be taken from either the gauss meter, 33120A function generator or the step down transformer. The reference signals from the gauss meter and the function generator are in the limits, that the DSP lock in can take. The line voltage is high and so the step down is used to lower the voltage levels. An intermediate circuit is placed between the step down transformer and the reference signal input. A SR540 chopper is placed between the laser rod and the first PBS to chop the light at required frequencies. In some setups the chopper is used while in other the chopper is not used.

Setup 2

The circular magnetic core is used. It is a laminated T02091XX1 Toroid core for electro core Inc [27]. We have cut a 14mm air gap in the circular core. An insulated higher order gauge wire is used, for winding it 360 turns around the circular magnetic core. This coil when excited by current generates the magnetic field across the air gap and it works like a current transformer. The sensor glass SF 57 is placed in air gap of the circular core where the magnetic field is produced by connecting the coil to a variac. The variac controls the flow of current in the CT's coil. A protective circuit [Figure 33] is placed between the variac and CT's coil, to short circuit any electrical surges or peaks. Either a 4.7Ω 6.2W or the 100Ω 100W resistor is place in series, with a capacitor, transient suppressor and the load in parallel. Changing the resistor helps us in getting a better dynamic range or better resolution. An ammeter is also place in series, to calculate the current flowing through the coil. A volt meter is place across the variac to calculate the voltage. The units of current and voltage are in amperes and volts respectively.

The Hall probe of the Lakeshore DSP 455 gauss meter is placed in the air gap of the CT. The magnetic field produced in the air gap of the CT is displayed on the gauss meter. The gauss meter is kept in auto range mode. The RMS value of the magnetic field is taken at the gauss meter. The magnetic field B is calibrated in milli tesla (mT). The picture of experimental setup can be seen on the Figure 10. The laser light is being focused on to the first PBS (polarizer) through a 20A filter. From the first PBS, the light is incident on the SF57 prism sensor glass in the air gap of the CT. The laser light is

modulated by the magnetic field, and is then reflected back from the sensor prism on to the half wave plate. The half wave plate is rotated at an angle of 22.5 degrees. The laser light passes through the half wave plate and falls on the second PBS (analyzer). The laser light is split into vertical and horizontal components.

The light intensity of each component is converted into electrical signal by the two SM05PD1A photo diodes. The electrical signal from the two photo diodes are connected to the inputs of SR 830 DSP lock in amplifier. The DSP lock in amplifier displays the resultant magnitude in volts. The difference between the two photo diodes are calculated, when the DSP lock in is in A-B mode at the signal input. The settings at the lock in are set as follows. No line is applied at the filter setup. The time constant is set to 1s with 12 dB slope/oct. The sensitivity setup is adjusted by the auto gain function. The reserve is set to low noise. The channel one display is set to R (resultant) with no off set. The interface and others are set to default setting. The source at the reference is kept at the internal. The reference signal to the lock in is applied at the REF IN. The reference signal may be taken from either the gauss meter, 33120A function generator or the step down transformer. The reference signals from the gauss meter and the function generator are in the limits, that the DSP lock in can take. The line voltage is high and so the step down is used to lower the voltage levels. An intermediate circuit is placed between the step down transformer and the reference signal input. A SR540 chopper is placed between the laser rod and the first PBS to chop the light at required frequencies. In some setups the chopper is used while in other the chopper is not used.

Setup 3

The circular iron core is used. It is a laminated T02091XX1 Toroid core for electro core Inc [27]. We have cut a 14mm air gap in the circular core. An insulated higher order gauge wire is used, for winding it 360 turns around the circular magnetic core. This coil when excited by current generates the magnetic field across the air gap and it works like a current transformer. The sensor glass SF 57 is placed in air gap of the circular core where the magnetic field is produced by connecting the coil to a variac. The wire wound circular iron core with the sensor glass placed in the air gap, are place on a hot plate [Figure 29]. The variac controls the flow of current in the CT's coil. A protective circuit [Figure 33] is placed between the variac and CT's coil, to short circuit any electrical surges or peaks. Either a 4.7Ω 6.2W or the 100Ω 100W resistor is place in series, with a capacitor, transient suppressor and the load in parallel. Changing the resistor helps us in getting a better dynamic range or better resolution. An ammeter is also place in series, to calculate the current flowing through the coil. A volt meter is place across the variac to calculate the voltage. The units of current and voltage are in amperes and volts respectively.

The Hall probe of the Lakeshore DSP 455 gauss meter is placed in the air gap of the CT. The magnetic field produced in the air gap of the CT is displayed on the gauss meter. The gauss meter is kept in auto range mode. The RMS value of the magnetic field is taken at the gauss meter. The magnetic field B is calibrated in milli tesla (mT). The laser light is being focused on to the first PBS (polarizer) through a 20A filter. From the

first PBS, the light is incident on the SF57 prism sensor glass in the air gap of the CT. The laser light is modulated by the magnetic field, and is then reflected back from the sensor prism on to the half wave plate. The half wave plate is rotated at an angle of 22.5 degrees. The laser light passes through the half wave plate and falls on the second PBS (analyzer). The laser light is split into vertical and horizontal components.

The light intensity of each component is converted into electrical signal by the two SM05PD1A photo diodes. The electrical signal from the two photo diodes are connected to the inputs of SR 830 DSP lock in amplifier. The DSP lock in amplifier displays the resultant magnitude in volts. The difference between the two photo diodes are calculated, when the DSP lock in is in A-B mode at the signal input. The settings at the lock in are set as follows. No line is applied at the filter setup. The time constant is set to 1s with 12 dB slope/oct. The sensitivity setup is adjusted by the auto gain function. The reserve is set to low noise. The channel one display is set to R (resultant) with no off set. The interface and others are set to default setting. The source at the reference is kept at the internal. The reference signal to the lock in is applied at the REF IN. The reference signal may be taken from either the gauss meter, 33120A function generator or the step down transformer. The reference signals from the gauss meter and the function generator are in the limits, that the DSP lock in can take. The line voltage is high and so the step down is used to lower the voltage levels. An intermediate circuit is placed between the step down transformer and the reference signal input. A SR540 chopper is placed between the laser rod and the first PBS to chop the light at required frequencies. In some setups the chopper is used while in other the chopper is not used.

Setup 4

The circular iron core is used. It is a laminated T02091XX1 Toroid core for electro core Inc [27]. We have cut a 14mm air gap in the circular iron core and placed the SF 57 sensor glass. A welding cable or a ¾ inch high tension cable is used in closed loop as the current carrying conductor. The current in the conductor loop is generated by placing either one or three of the current transformer. The Model 195-202 metering class CT is used with current ratio of 2000:5 from Flex-Core [34]. These CTs are actually designed to calculate the current flowing through the conductor by detecting the magnetic field, but they are being used in the reverse mode. The current is applied to the CTs and they produce the magnetic field; and this field will in turn produce the current in the conductor loop that is passing through the CTs. The CTs are connected in parallel to the variac that control the current in the loop. Either a single or a double loop setup is used which passes through the circular iron core that generates the magnetic field; one or three metering class CTs that generate current; and another metering class CT that calculates the current (the ammeter in the loop – normal mode of the CT) in the loop [Figure 25]. An ammeter is also place in series, to calculate the current flowing through the coils of the CTs. A volt meter is place across the variac to calculate the voltage. The units of current and voltage are in amperes and volts respectively.

The hall probe of the Lakeshore DSP 455 gauss meter is placed in the air gap of the CT. The magnetic field produced in the air gap of the CT is displayed on the gauss meter. The gauss meter is kept in auto range mode. The RMS value of the magnetic field

is taken at the gauss meter. The magnetic field B is calibrated in milli tesla (mT). The laser light is being focused on to the first PBS (polarizer) through a 20A filter. From the first PBS, the light is incident on the SF57 prism sensor glass in the air gap of the CT. The laser light is modulated by the magnetic field, and is then reflected back from the sensor prism on to the half wave plate. The half wave plate is rotated at an angle of 22.5 degrees. The laser light passes through the half wave plate and falls on the second PBS (analyzer). The laser light is split into vertical and horizontal components.

The light intensity of each component is converted into electrical signal by the two SM05PD1A photo diodes. The electrical signal from the two photo diodes are connected to the inputs of SR 830 DSP lock in amplifier. The DSP lock in amplifier displays the resultant magnitude in volts. The difference between the two photo diodes are calculated, when the DSP lock in is in A-B mode at the signal input. The settings at the lock in are set as follows. No line is applied at the filter setup. The time constant is set to 1s with 12 dB slope/oct. The sensitivity setup is adjusted by the auto gain function. The reserve is set to low noise. The channel one display is set to R (resultant) with no off set. The interface and others are set to default setting. The source at the reference is kept at the internal. The reference signal to the lock in is applied at the REF IN. The reference signal may be taken from either the gauss meter, 33120A function generator or the step down transformer. The reference signals from the gauss meter and the function generator are in the limits, that the DSP lock in can take. The line voltage is high and so the step down is used to lower the voltage levels. An intermediate circuit is placed between the step down transformer and the reference signal input. A SR540 chopper is placed

between the laser rod and the first PBS to chop the light at required frequencies. In some setups the chopper is used while in other the chopper is not used.

REFERENCES

[1] S T Pai, C M Luo, J Song and G X Zhang, “Magneto-optical current sensors constructed with ZF glass,” Sensors and Actuators A, 35 (1992) 107-112, Elsevier Sequoia(1991).

[2] Gerhard Westenberger, Hans J. Hoffmann, Werner W. Jochs, and Gudrun Przybilla, “The Verdet constant and its dispersion in optical glasses,” Passive Materials for Optical Elements (1991) / 113,No 0-8194-0663-5/91,SPIE Vol. 1535.

[3] Paper presented jointly by Emerging Technologies Working Group and Fiber Optic Sensors Working Group, “ Current transducers for power systems: a review,” IEEE Transactions on Power Delivery, Volume 9, Issue 4, Oct. 1994 Page(s):1778 – 1788, Digital Object Identifier 10.1109/61.329511.

[4] J.W. Dawson, T.W. MacDougall and E. Hernandez,”Verdet constant limited temperature response of a fiber-optic current sensor,” IEEE Photonics Technology Letters, Volume 7, Issue 12, Dec. 1995 Page(s):1468 – 1470, Digital Object Identifier 10.1109/68.477285.

[5] Mihailovic, P.; Petricevic, S.; Stojkovic, Z. and Radunovic, J.B., ”Development of a portable fiber-optic current sensor for power systems monitoring,” IEEE Transactions on Instrumentation and Measurement, Volume 53, Issue 1, Feb. 2004 Page(s):24 – 30, Digital Object Identifier 10.1109/TIM.2003.821500.

[6] Yi, B.; Chu, C.B.; Chiang, K.S. and Chung, H.S.H., “New design of optical electric-current sensor for sensitivity improvement,” IEEE Transactions on Instrumentation and Measurement, Volume 49, Issue 2, April 2000 Page(s):418 – 423, Digital Object Identifier 10.1109/19.843089.

[7] Gongde Li; Kong, M.G.; Jones, G.R. and Spencer, J.W., “Sensitivity improvement of an optical current sensor with enhanced Faraday rotation,” Journal of Lightwave Technology, Volume 15, Issue 12, Dec. 1997 Page(s):2246 – 2252, Digital Object Identifier 10.1109/50.643549.

[8] Chen C L, Asars J A and Vaerwyck E G, “Temperature compensated current sensor involving,” Faraday effect and fibre optics 1985, UK Patent 8520392.

[9] Vaerewyck E G. Chen G L and Asars J A, “ Faraday current sensor with fiber optic compensated by temperature, degradation and linearity,” US Patent 4613 81 1.

[10] Chen C L, Asars J A and Vaerewyck E G, “Temperature stabilized Faraday rotator current sensor by Thermal mechanical means,” 1986, US Patent 4612500.

[11] Katsukawa, H.; Ishikawa, H.; Okajima, H.; Cease, T.W, “Development of an optical current transducer with a bulk type Faraday sensor for metering,” IEEE Transactions on Power Delivery, Volume 11, Issue 2, Apr 1996 Page(s.):702 – 707, Digital Object Identifier 10.1109/61.489326.

[12] S H Zaidi et al, “Faraday-effect magnetometry: compensation for the temperature-dependent Verdet constant,” 1994 Meas. Sci. Technol. 5 1471-1479, DOI: 10.1088/0957-0233/5/12/008.

[13] Nobukazu Inoue and Kazuhito Yamasawa, “Stabilization of temperature dependence of Verdet constant of bi-doped garnet and development of high sensitive optical fiber magnetic field sensor,” DOI: 10.1002/eej.4391170101.

[14] Erning L.; MacAlpine J.M.K.1; Yanbing L. and Benshun Y, “A novel optical current transducer for power systems,” DOI: 10.1016/S0378-7796(98)00031-5.

[15] Jay N Damask, Inc,”Polarization Optics in Telecommunications,” Net Library Springer, 2005.

[16] Eugene Hecht, “Faraday effect,” HECHT OPTICS 2nd edition, ISBN 0-201-11609-X

[17] "Faraday effect." Encyclopædia Britannica. 2008. Encyclopædia Britannica Online. 10 Sep. 2008 <http://www.britannica.com/EBchecked/topic/201736/Faraday-effect>.

[18] "Polarization." Encyclopædia Britannica. 2008. Encyclopædia Britannica Online. 08 Sep. 2008 <http://www.britannica.com/EBchecked/topic/467121/polarization>.

[19] Gerd keiser, “Laser,” Optical Fiber Communications, Page 141, McGraw-Hill, 2000 ISBN 0072321016, 9780072321012.

[20] Bahaa E. A. Saleh and Malvin Carl Teich ,“Polarizer and Polarization rotators,” Fundamentals of Photonics, Page 230 – 233, Published by Wiley-Interscience, 2007 ISBN 0471358320, 9780471358329

[21] Bahaa E. A. Saleh and Malvin Carl Teich ,“Total internal reflection,” Fundamentals of Photonics, Page 11, Published by Wiley-Interscience, 2007 ISBN 0471358320, 9780471358329

[22] Eugene Hecht, “Porro prism, Half wave plate”, HECHT OPTICS 2nd edition. Page 167, 270 and 316, ISBN 0-201-11609-X

[23] Schott datasheet, <http://www.us.schott.com/optics_devices/english/download/datasheet_all_us.pdf?PHPSESSID=eu00t79kuf3r48h1b0nhe6a3v4>

[24]The SR830 DSP Lock in amplifier Operation Manual, <http://www.thinksrs.com/downloads/PDFs/Manuals/SR830m.pdf>

[25] The Lakeshore DSP Gauss meter 455 Manual, <http://www.eastchanging.com/admin/cxsb/gaussmeter/455.pdf>

[26] The SR540 Chopper Manual, http://facilities.mrl.uiuc.edu/laserlab/manuals/SR540m.pdf

[27] Toroid T02091XX1 Products, <http://www.electro-core.com/products.htm>

[28] Split core CT, <http://www.flex-core.com/pdf-files/New%20pdf%20files/Page12%20Model%20331%20Current%20Transformer.pdf>

[29] Law of refraction, <http://fis.cie.uma.es/old/docencia/2002-03/A109/links/uwinnipeg/physics/light/img21.gif>

[30] Linear Polarization, <http://www.lw4u.com/images/LI3d.gif>

[31] Circular Polarization, <http://www.tau.ac.il/~phchlab/experiments/Sucrose/What%20d28.gif>

[32] Porro Prism, <http://en.wikipedia.org/wiki/Image:Porro-prism.png>

[33] The Polarization beam splitting of light, <http://www.opticsshop.com.au/images/pbs1.gif>

[34] Current transforms datasheet, <http://www.flex-core.com/pdf-files/New%20pdf%20files/Page25%20Model%20191-194-195%20Current%20Transformer.pdf>

[35] Anders E. Petersen,"Portable optical AC- and proposed DC-current sensor for high voltage applications," IEEE Transactions on Power Delivery, Volume 10, Issue 2, April 1995 Page(s):595 – 599, Digital Object Identifier 10.1109/61.400873